

INFORMATION TO USERS

This material was produced from a microfilm copy of the original document. While the most advanced technological means to photograph and reproduce this document have been used, the quality is heavily dependent upon the quality of the original submitted.

The following explanation of techniques is provided to help you understand markings or patterns which may appear on this reproduction.

1. The sign or "target" for pages apparently lacking from the document photographed is "Missing Page(s)". If it was possible to obtain the missing page(s) or section, they are spliced into the film along with adjacent pages. This may have necessitated cutting thru an image and duplicating adjacent pages to insure you complete continuity.
2. When an image on the film is obliterated with a large round black mark, it is an indication that the photographer suspected that the copy may have moved during exposure and thus cause a blurred image. You will find a good image of the page in the adjacent frame.
3. When a map, drawing or chart, etc., was part of the material being photographed the photographer followed a definite method in "sectioning" the material. It is customary to begin photoing at the upper left hand corner of a large sheet and to continue photoing from left to right in equal sections with a small overlap. If necessary, sectioning is continued again -- beginning below the first row and continuing on until complete.
4. The majority of users indicate that the textual content is of greatest value, however, a somewhat higher quality reproduction could be made from "photographs" if essential to the understanding of the dissertation. Silver prints of "photographs" may be ordered at additional charge by writing the Order Department, giving the catalog number, title, author and specific pages you wish reproduced.
5. PLEASE NOTE: Some pages may have indistinct print. Filmed as received.

Xerox University Microfilms

300 North Zeeb Road
Ann Arbor, Michigan 48106

76-19,683

SIEGELL, Jeffrey Howard, 1950-
DEFLUIDIZATION PHENOMENA IN FLUIDIZED BEDS
OF STICKY PARTICLES AT HIGH TEMPERATURES.

City University of New York, Ph.D., 1976
Engineering, chemical

Xerox University Microfilms, Ann Arbor, Michigan 48106

DEFLUIDIZATION PHENOMENA
IN
FLUIDIZED BEDS
OF
STICKY PARTICLES
AT
HIGH TEMPERATURES

by
JEFFREY HOWARD SIEGELL

A dissertation submitted to the Graduate
Faculty in Engineering in partial fulfillment
of the requirements for the degree of Doctor
of Philosophy.

The City University of New York

1976

This manuscript has been read and accepted for the Graduate Faculty in Engineering in satisfaction of the dissertation requirement for the degree of Doctor of Philosophy.

23 April 1976
Date

Robert A. Graff
Chairman of Examining Committee

April 23, 1976
Date

Jacques E. Benveniste
Executive Officer

Prof. Robert A. Graff (Chairman)

Prof. Leslie L. Isaacs

Prof. Arthur M. Squires

Prof. Joseph Yerushalmi

The City University of New York

ACKNOWLEDGEMENTS

I acknowledge my dept to my research advisors for their constant support and inspiration; Drs. Michael J. Gluckman, Robert A. Graff, Leslie L. Isaacs, Morris Kolodney, Arthur M. Squires and Joseph Yerushalmi.

I am grateful to the National Science Foundation for the RANN(Research Applied to National Needs) Grant No. AER-72-03426#4(formerly GI-34286) that supported this research and, for my personal support through an Energy Related Graduate Traineeship; to E. I. duPont de Nemours for the photomicrographs and electron micrographs of the agglomerates; to American Electric Power, Institute of Gas Technology and Commonwealth Edison for providing coal ash.

No experimental program could be completed without an efficient technical support staff. For this I thank Mr. John Bodnaruk and the members of the Chemical Engineering Shop.

TABLE OF CONTENTS

	page
1. BACKGROUND OF AGGLOMERATING FLUIDIZED BEDS	1
1.1 Fuller's Process for Cement	1
1.2 The Ignifluid Boiler	3
1.3 Other Agglomerating Beds	5
1.4 Applications of Agglomerating Beds Forming Beads	5
1.5 Difficulties with Defluidization in Two Developments	7
1.6 Agglomeration in the Ignifluid Boiler	9
2. POTENTIAL APPLICATIONS OF PARTICLE AGGLOMERATION TO COAL TECHNOLOGY	11
2.1 Application of Agglomeration Due to Sintering	11
2.2 Rational of Current Studies	12
2.3 Subject of Research	13
2.4 Advantage of Agglomeration in Fluidized Beds	13
3. SINTERING	15
3.1 Material Transport by Diffusion	17
3.2 Material Transport by Viscous Flow	19
3.3 Material Transport by Vapor Transfer	21
3.4 Summary of Sintering Rate Equations	23
3.5 Stages of Sintering	23
4. BEHAVIOR OF COAL ASH AT HIGH TEMPERATURES	25
4.1 Determination of Coal Ash Sintering Temperatures	29
5. EXPERIMENTAL APPARATUS AND METHOD	31
5.1 Experimental Equipment	31
5.2 Sample Preparation	34

5.3	Determination of Defluidization	35
5.4	Determination of an Initial Sticky Temperature	36
5.5	Determination of Minimum Fluidization Velocities	38
5.6	Temperature Profiles in Six Inch Bed ...	40
6.	EXPERIMENTAL RESULTS	43
7.	DEFLUIDIZATION MODEL	52
8.	CONCLUSIONS	60
APPENDIX I:	FIGURES	65
APPENDIX II:	DEFLUIDIZATION DATA	102
APPENDIX III:	COAL ASH COMPOSITIONS	126
APPENDIX IV:	COEFFICIENTS FOR DEFLUIDIZATION CURVES	127
APPENDIX V:	AGGLOMERATE EXAMINATION	128
APPENDIX VI:	HIGH SPEED PHOTOGRAPHY	148
REFERENCES	152
VITA	156

LIST OF FIGURES

	page
I. Temperature - Velocity Relationship for Defluidization	66
II. Indirectly Heated Equipment	67
III. Directly Heated Equipment	68
IV. Details of Directly Heated Equipment	69
V. Defluidization Point Determination	70
VI. Temperature Profiles of Six Inch Beds	71
Experimental Results	
VII. Copper -16+20 U.S. Sieve	73
VIII. Copper -20+30 U.S. Sieve	74
IX. Copper -40+50 U.S. Sieve	75
X. Polyethylene Beads	76
XI. Polyethylene Balls	77
XII. Lexan Beads	78
XIII. Polypropylene Beads	79
XIV. Dacron Beads	80
XV. Glass -14+16 U.S. Sieve	81
XVI. Glass -16+18 U.S. Sieve	82
XVII. Coal Ash (AEP) -16+20 U.S. Sieve	83
XVIII. Coal Ash (AEP) -20+30 U.S. Sieve	84
XIX. Coal Ash (AEP) -30+40 U.S. Sieve	85
XX. Coal Ash (AEP) -40+50 U.S. Sieve	86
XXI. Coal Ash (IGT) -16+20 U.S. Sieve	87
XXII. Coal Ash (IGT) -20+30 U.S. Sieve	88
XXIII. Coal Ash (IGT) -30+40 U.S. Sieve	89
XXIV. Coal Ash (IGT) -40+50 U.S. Sieve	90
XXV. Coal Ash (CE) -16+20 U.S. Sieve	91
XXVI. Coal Ash (CE) -20+30 U.S. Sieve	92
XXVII. Coal Ash (CE) -30+40 U.S. Sieve	93
XXVIII. Coal Ash (CE) -40+50 U.S. Sieve	94
XXIX. Polyethylene Beads L/D	95
XXX. Glass Spheres	96
XXXI. Sintering Studies - Copper	96
XXXII. Sintering Studies - Polymers	97
XXXIII. Sintering Studies - Glass	98
XXXIV. Silicon Carbide - Glass Mixtures	99
XXXV. Sintering Studies - Coal Ash	100
XXXVI. T_s vs. T_s'	101

LIST OF AGGLOMERATE PHOTOGRAPHS AND MICROGRAPHS

	page
1. Copper Agglomerate	136
2. Copper Agglomerates	136
3. Copper Bonding Zone	137
4. Copper Bonding Zone	137
5. Copper Bonding Zone	138
6. Copper Bonding Zone	138
7. Glass Agglomerate	139
8. Glass Agglomerate	139
9. Glass Agglomerate	140
10. Glass Agglomerate	140
11. Glass Bonding Zone	141
12. Glass Bonding Zone	141
13. Polyethylene Sphere Bonding Zone	142
14. Polyethylene Sphere Bonding Zone	142
15. Polyethylene Bead Bonding Zone	143
16. Polyethylene Bead Bonding Zone	143
17. Polypropylene Agglomerate	144
18. Polypropylene Agglomerate	144
19. Coal Ash Agglomerate	145
20. Coal Ash Agglomerate	145
21. Coal Ash Agglomerate	146
22. Coal Ash Agglomerate	146
23. Coal Ash Agglomerate	147
24. Coal Ash Agglomerate	147

1. BACKGROUND OF AGGLOMERATING FLUIDIZED BEDS

The past twenty years has seen an emergence of at least two new technologies for agglomerating materials in fluidized beds. In one species of agglomerating bed, the solid product is in form of dense, spherical pellets or beads. In another, the solid product consists of a loose, friable agglomerate of relatively high porosity. The two types of beds will first be illustrated by examples, and later the principles of their operation will be considered in greater detail.

1.1 Fuller's Process for Cement

Fuller Company has piloted an agglomerating bed for the manufacture of cement (Kramer, 1961; Sadler, 1967; Pyzel, 1957, 1959, 1961a, 1961b). The cement product is in the form of "beads", that is to say nearly spherical, dense, nonporous particles which bear little physical resemblance to the usual cement klinker. A carefully sized bed of ordinary clinker is used in the startup of Fuller's process, but the bed quickly becomes altered to the bead form, as the original startup material is gradually discharged along with product.

Heat for the process is supplied by combustion of fuel oil with air and the heat requirements and fluidization velocity determine the size of the bed. Oil is fed to the bed at four points only and, during operation of the pilot unit, the combustion of the oil often momentarily took place in the freeboard above the bed. This caused no serious trouble in the pilot unit but more oil inlets would probably be furnished in a commercial plant.

Raw materials for cement are clay, lime-

stone and sometimes a little iron ore. These raw materials, in any cement process, must be finely ground to promote their intimate mutual contact during the reactions which yield cement.

In Fuller's process, the raw materials are introduced via a central 4-inch pipe into the bottom of the fluidized bed. The bed, within a few hours after startup, comprises beads of the cement product. In the bed, the raw materials are heated almost instantaneously to the temperature of the bed, and quickly react to make new cement. This adheres to the beads of cement made earlier, which accordingly grow in size. Product is continuously discharged by overflow, is screened and undersized material is returned to the bed.

The basis of the process is the fact that intermediate products formed by the reacting solid materials are molten. Blanks and Kennedy (1955) state that a liquid phase begins to form, in a conventional cement-making rotary kiln, as the raw solids pass the point at which the temperature is about 2300°F. A common problem in operating a cement kiln is that of preventing a ring of material from accumulating at this point and blocking the kiln. In Fuller's process, which operates a little below 2400°F, the raw materials apparently form a melt, which produces smears of liquid upon beads, which happen to be in the vicinity of the inlet for the raw solids. The smears quickly react to form dry cement product. The net effect is that these beads grow a little in size. Because of the good mixing of solids in the fluidized bed, the rate of growth of beads, throughout the bed, is substantially uniform when the rate is viewed over several minutes of time.

In effect, the fluidized bed of cement

beads acts as a "dust trap" for the cement raw materials, the effectiveness of the trap arising from the fact that the raw materials pass through a molten phase on their way to cement. Carryover of solids from the bed is remarkably small, amounting to only a few percent of daily production (Kramer, 1961). Furthermore, much of the carryover is large in size and is a result of geysering caused by the aforementioned occasional burping of oil at the surface of the bed. Carryover almost vanishes if the oil is turned off and there is no evidence that much attrition of the cement beads occurs. Carryover that is small in particle size typically comprises tiny spherical matter of about 2 to 5 microns, and it is significant that this material is cement and not particles of calcined raw solids. Indeed, a remarkable feature of the product of Fuller's process is the complete absence of free lime. Carryover is returned to the bed as seed for growth of new beads.

It should be remarked that Fuller Company has not been successful in marketing its new cement process. This circumstance does not appear to result from a fault of the agglomerating fluidized bed, which is said to have operated smoothly during extensive pilot tests. The principal problems, during the development, involved the metallurgy of heat-exchange tubes transferring heat from flue gas to incoming air. It would appear that the main difficulty in marketing the process has been an unduly large fuel requirement. During Fuller's development, significant improvements were made in the fuel economy of the conventional kiln system for cement.

1.2

The Ignifluid Boiler

A second type of agglomerating bed produces a loose, friable agglomerate. Godel (1958, 1966)

exploits the second type in his Ignifluid boiler, now marketed by Babcock-Atlantique of France (Cosar, 1969). This boiler is now operating at the 25-megawatt scale.

A fluidized bed, comprising mainly coke, sits upon a travelling grate. The bed is at about 2300^oF, and coal fed to the bed at $\frac{3}{4}$ inch is quickly devolatilized to form particles of coke. The bed is fluidized with air at about 40 ft/sec, the air rate being approximately 60% of the stoichiometric quantity required for complete combustion of the coal. The coke is gasified to yield a fuel gas resembling producer gas, probably having a heating value between about 80 and 100 Btu/SCF. Normally no steam is added, and so the bed must lose an appreciable amount of heat by radiation from its upper surface to the tubes in the upper part of the boiler. The gas is burned above the fluidized bed by injecting secondary air.

Godel made the remarkable and important discovery that ash-matter of substantially all coals is self-adhering at a temperature above about 2000^oF. More than 18 coals of a wide range of types have been examined (Godel, 1968). In the Ignifluid boiler the fluidized bed is rich in carbon and lean in ash matter. As a coke particle is gasified ash is released, ash sticks to ash and not to coal, and ash agglomerates form. These sink to the grate, are captured by a "sticky" pad of ash, and are carried to an ash pit. For most coals, substantially complete carbon burnup is achieved simply by returning the particles carried out of the boiler to the fluidized bed. Such particles are relatively coarse and are easy to collect.

The upper regions of an Ignifluid boiler are reported to resemble a gas-fired boiler (Demmy, 1971),

free of the deposits so characteristic of the combustion zone of a conventional pulverized-fuel furnace.

A detailed analysis, of the formation of ash agglomerates in the Ignifluid boiler, has been presented by Yerushalmi (1975).

In summary, the agglomeration and growth of ash particles in the Ignifluid boiler is the result of softening of the glassy portion of the ash, to form a sticky viscous fluid that is self-adhering.

1.3 Other Agglomerating Beds

Ash agglomerates produced in experiments in coal combustion at Battelle Memorial Institute (Goldberger 1967; Stephens and Goldberger, 1965) were dense beads similar to those produced by the Fuller Cement Process.

Ash agglomerates produced in a coal gasification pilot plant at Centre d'Etudes et Recherches des Charbonnages de France (Jequier, Longchambon and Van de Putte, 1960) would appear to represent matter which began as a loose agglomerate of the general type made by Godel. Godel's agglomerates sink rapidly to his traveling grate and are carried away from the fluidized bed. In The Battelle and CHERCHAR arrangements, the agglomerates themselves are fluidized for an appreciable length of time at temperatures such that further sintering and melting, or consolidation occurs, so that a denser ash particle results.

1.4 Applications of Agglomerating Beds Forming Beads

For nearly 25 years, Door-Oliver has calcined finely divided CaCO_3 to produce pellets of lime.

The CaCO_3 arises either from causticizing green liquor from paper-making, or from water treatment. Dorr-Oliver also roasts sulfide ore concentrates in agglomerating beds, and burns paper industry waste liquor in the presence of SO_2 to produce pellets containing Na_2CO_3 and Na_2SO_4 (Angvine, 1971).

An application has been studied on the bench scale at Battelle Memorial Institute (Langston and Stephens, 1960; Stephens, Coffey and Langston, 1962). Pulverulent iron oxide, smaller than -325 mesh, was injected into a bed of iron shot, suitably about 1/8 inch in diameter, fluidized by hydrogen at a temperature greater than about 1400°F and at velocities as high as 35 ft/sec. The iron oxide was reduced and the resulting tiny particles of iron were captured by the shot. Iron is not normally regarded as "sticky" at temperatures in the vicinity of 1400°F , but the fresh iron particles evidently "plate out" upon the iron shot by a mechanism which might be termed "contact welding".

1.5 Difficulties with Defluidization in Two Developments

The effort to develop fluidized-bed reactors for Fischer-Tropsch synthesis in 1946 ran into difficulties, due to bed defluidization problems which apparently arose from a tendency of the particles to agglomerate. The particles were small in size, usually smaller than -20 mesh, and with an appreciable content of material smaller than -325 mesh.

When iron oxide powder was reduced with hydrogen, at about 15 atmosphere to provide catalyst for such reactors, it was found that many iron powders could not be fluidized with hydrogen at temperatures even as low as 700°F. Out of this effort came Hydrocarbon Research, Inc.'s "H-Iron" Process (Squires and Johnson, 1957; Squires, 1968a; Squires 1969c), in which iron ore is reduced by hydrogen at about 35 atm and 900°F.

Work on the "H-Iron" development revealed that larger particle size, lower temperature, higher velocity and higher gangue content tended to favor stable fluidization. The impression was gained that a sharp boundary exists in the space defined by these variables between a region in which stable fluidization can be reliably achieved and a region in which stable fluidization cannot occur.

For example, if a given powdered iron is fluidized at a certain temperature and the velocity is reduced, often a velocity is reached at which the bed "drops dead", as shown in Figure I, although this velocity may be well above the theoretical minimum for fluidization of the powder. If the velocity is raised again, the bed recovers provided it has not been allowed to remain too long in the slumped condition. The velocity marking the boundary between stable fluidization and the slumped condition appears

precise for a given powder and a given temperature. When the bed is in the slumped condition, the gas tends to pass upward through the bed in well-defined chimneys, termed "rat-holes" at Hydrocarbon Research.

Similarly, if the velocity is held constant and the temperature raised, the temperature at which the bed slumps is also remarkably precise. A lowering of temperature serves to restore the bed to the fluidized condition if it has not been held at a higher temperature too long, or if the higher temperature has not been too hot.

Although the experiment could not be performed, it seems probable that a slumped bed could be restored if it were possible to cause a small increase in average particle size or gangue content.

The iron powder produced in the H-Iron Process is an active iron of high internal surface area and porosity. The tendency of the bed material to agglomerate was overcome by reducing the temperature and then increasing the yield by increasing the pressure. Hydrocarbon Research, Inc. is reported to have conducted fluidization experiments with spherical copper shot where this material displayed similar behavior to that just described for the active iron being reduced. Defluidization temperature for copper shot were said to be lower even than for iron.

In first attempts at Hydrocarbon Research to gasify anthracite "silt", the fine wastes from anthracite mining and cleaning, clinkers formed under circumstances which strongly implied defluidization behavior similar to that seen earlier with iron. A clinker was loosely sintered on the outside, but showed signs of having reached progressively higher temperature toward the middle, which was often semi-fused, indicating that a temperature had

been reached well over 2,850°F, the softening temperature of the ash of the anthracite silt undergoing gasification. The clinker had formed in a fluidized bed operating at a temperature below 1,700°F. It appeared that initially a portion of the bed had defluidized and that oxygen had subsequently diffused into the region of slumped powder.

Fluidization studies were undertaken on the ash and the studies gave data which tended to confirm this inference. As in the case of the iron powder and the copper shot, a sharp boundary between a region of active fluidization and a slumped condition was observed (see Figure I). The boundary was at lower velocities at higher levels of carbon upon the ash. It should be noted that the temperatures of the experiments were below 2,000°F, although the initial deformation temperature of the ash was 2,650°F.

Raising the velocity was recognized as a cure to the clinkering problem. This was done and successful gasification trials were conducted in a large pilot unit (Squires, 1961).

1.6 Agglomeration in the Ignifluid Boiler

The Hydrocarbon Research experience sheds light upon the coal-ash agglomerating phenomenon discovered and exploited by Godel in the Ignifluid boiler. The bed in this boiler comprises primarily relatively large particles of coke, since the fluidizing-gas velocity of 10 ft/sec is too high for small particles to remain very long in the bed. We can speculate that the carbon in recycled fines must be consumed only after the fines have made several quick trips through the bed. Ash matter nevertheless, finds other ash matter to become bonded together by forces which probably arise from chemical phenomena similar to those which caused

the defluidization in the Hydrocarbon Research experiments. The temperature in the Ignifluid boiler's bed is generally about 100°F to 200°F above the temperatures which caused defluidization of anthracite ash in the experiments, and so the bonding of the Ignifluid ash agglomerates is probably much stouter than in the slumped powder of ash in the Hydrocarbon Research tests. It should perhaps be emphasized again that the defluidization boundary could be crossed back and forth many times, either by lowering and raising velocity or by lowering and raising temperature, with the bed recovering fluidity each time the "active fluidization" region is entered, provided the bed has not been left in the "dead" region too long. The bridges which cause defluidization of a fine powder can apparently be exceedingly weak.

2. Potential Applications of Particle Agglomeration to Coal Technology

Some examples of new applications of the principles of particle agglomeration to the design of coal processing equipment will be discussed below.

2.1 Application of Agglomeration Due to Sintering

What are the important lessons to be learned from the previously cited examples of agglomeration due to sintering? The tendency of coal ash to agglomerate, that plagued the anthracite gasification development program of H.R.I., teaches that fluidized beds containing mixtures of agglomerating (ash) and non-agglomerating (coke) particles exhibit an unfortunate tendency to slump or defluidize at high temperature and low velocity. Albert Godel overcame this dangerous tendency of a fluidized bed to slump simply by increasing the velocity by an order of magnitude. Not only did he overcome the defluidization problem, but he actually exploited the agglomerating properties of the ash material to devise a simple and essentially fool-proof ash removal scheme.

Dent (1958, 1971) reported that a fluidized - bed gasifier, working at atmospheric pressure and 1,920°F, can yield gas which is substantially at equilibrium for the steam-carbon reaction. In light of this report, a fluidized bed broadly of the type developed for the Ignifluid boiler would appear to be a strong candidate for use at elevated pressure to gasify coal char or coal. It would probably no longer be practicable to discharge ash agglomerates by means of a moving grate, but other means to discharge ash appear feasible for use at high pressure. Gasification could be with oxygen and steam in a system producing pipeline gas or industrial gas, or it could be with

air and steam, to provide a lean fuel gas for generating power in gas turbines.

One of the major questions concerning a gasifier of the above description that cannot be answered at this time, is what concentration of ash matter can an ash agglomerating fluidized bed tolerate at any particular conditions of temperature and velocity without undergoing the risk of defluidization? The research in this area was aimed at answering the above question in a qualitative manner.

Squires (1969a, 1971b) has called attention to the opportunity to carbonize or hydrocarbonize coal in a coke-self-agglomerating bed. Finely divided coal would be supplied to a bed of coke pellets maintained at a temperature above about 1100°F, to be heated therein and almost instantaneously decomposed into a gaseous fraction, mainly methane and hydrogen, and a sticky, semi-fluid residue. The latter would adhere to a coke pellet, forming a smear. Further polymerization and coking reactions, which occur in the order of a second (Hiteshue, Friedman and Madden, 1964), would transform the sticky smear into dry coke, while additional gases evolve.

One application of the coke-self-agglomerating bed would be production of coke beads low in sulfur simultaneously with production of a low-sulfur fuel gas for power generation (Squires, 1969b; Squires, Graff, and Pell, 1969).

2.2 Rationale of Current Studies

Although exciting commercial applications have arisen, and suggestive pilot studies reported, it is believed many additional opportunities exist for agglomerating beds which would perhaps already be under development if there were more general knowledge of the principles which

govern these beds. Little exists yet in the open literature concerning such principles, and indeed, there is not yet a general understanding or agreement upon them even among persons having some experience with agglomerating beds. This absence may well be due to the fact that at least three species of agglomerating beds exist as we have seen. Yet I believe the principles, which underly all agglomerating technologies, to be essentially the same.

Absence of understanding leads to timidity in assaying new developments for applications of agglomerating beds. Even qualitative information, clearly established, could be of great value at this point in providing the spark to get several potentially valuable developments in coal technology underway.

2.3 Subject of Research

This research was limited to agglomerating beds due to the sintering of the bed material at elevated temperature. Agglomeration due to the addition of a sticky substance to a fluidized bed at normal temperature has been studied by Cankurt (1974, 1975).

2.4 Advantage of Agglomeration in Fluidized Beds

If the developer of a fluidized-bed process using a fine powder encounters defluidization difficulties, let him consider as an alternative the development of an agglomerating-bed process using a coarse solid fluidized at a much higher velocity.

The agglomerating tendency of iron powder, which plagued the H-Iron development, was exploited by the workers at Battelle, in their agglomerating bed of iron shot. The increase in fluidization velocity, and hence in capacity,

from this change in direction of effort was more than 20-fold.

The agglomerating tendency of coal ash, which plagued the anthracite gasification development, was exploited by Godel, with a nearly 10-fold increase in fluidization velocity and capacity.

The agglomerating tendency of bituminous coal undergoing carbonization is a property to exploit rather than to struggle against, as in prior efforts to develop fluidized-bed processes for carbonizing or hydrocarbonizing coal. An increase in capacity of 10-fold or more can be expected.

A catalog of examples would encourage development agglomerating bed technologies even in absence of knowledge of the laws. In view of the experience sketched above, it appears probable that additional examples would reinforce the impression that defluidization phenomena obey precise laws. The examples might dispel timidity in tackling agglomerating-bed developments even before knowledge of the laws become available. In any case, it does not seem probable that the laws will be perceived until additional examples are available. Obtaining data for a number of well-defined systems was therefore the first major task of the current research.

The hope was that the research would encourage persons who contemplate development of an agglomerating-bed process. Such persons need courage for, even the initial experiment in such a development, must usually be conducted on a large and expensive scale.

3. Sintering

There is no single definition of sintering that is generally accepted by powder metallurgists. Many define it as migration of holes or lattice vacancies. Others prefer to describe it as motions of atoms to a less dense area of the material. Both of these definitions are essentially correct, depending upon how one wishes to consider the sintering mechanism. For the purpose of the current study it is not important to have a single definition, but simply to understand the effects on defluidization.

Consider two particles in a fluidized bed operating at elevated temperatures, but well below the melting temperature of the particle material. If these two particles come in contact with each other they will tend to join together into a single particle. The driving force for this will be a decrease in surface area and thus surface energy. Since the bed is fluidized, it is more than likely that the particles will contact with sufficient kinetic energy to break apart and overcome the forces attempting to bond them together. However, if the temperature of the bed is raised sufficiently so that the particles coming in contact will bond together overcoming their kinetic energy, the bed will defluidize. At this temperature of defluidization the material in the bed has still not reached its normal melting temperature. The energy needed to overcome the kinetic energy of the fluidized bed was due to an increased rate of sintering at the higher temperature.

Consider again the same two particles. If they are brought in contact with each other at room temperature, chances are they will never bond together. This is because, at room temperature, the rate of sintering is not sufficient

to allow material to migrate to the point of contact and form a bond. However, at higher temperatures the sintering rate increases so that these same two particles, when brought in contact, will tend to form a bond between them decreasing their surface area. If they remain at this high temperature they will eventually coalesce into a single dense particle of spherical shape because a sphere has the smallest surface energy for a given particle volume. The temperatures and time necessary for this phenomenon to occur depends on the particular material being considered.

The sintering process has been used industrially mainly in the production of strong fabricated materials from weakly bonded powders. These powders are usually compacted at room temperature, cold pressed, and then heated to a temperature high enough to promote sintering but well below the melting point. At this temperature, material begins to migrate toward the particle contact areas, forming stronger bonds. Eventually this sintering process begins to decrease the porosity of the compacted powder, increasing its mechanical strength.

Due to its importance as a manufacturing technique, this sintering process has been studied in great detail. At the present time, however, no complete quantitative theory exists to describe it. Considerable information has been developed with regard to the probable mechanisms by which material is transported during the sintering process. The importance of looking at sintering here is that it seems to be the process by which bonds are formed between particles in fluidized beds at high temperatures, causing these beds to defluidize.

The driving force for sintering, as was stated before, is a tendency for a powder to decrease its surface

area and thus its surface energy. The transport of material to the bond zones decreasing the surface area may take place by four generally accepted mechanisms; surface diffusion, volume diffusion, viscous flow and vaporization. These mechanisms are physically different from one another but they may all occur simultaneously. In cases where more than one mechanism of material transport occurs, there is usually a predominant mechanism depending on the nature of the system and the conditions under which it is sintering.

3.1 Material Transport by Diffusion

Sintering by diffusion involves the movement of atoms from regions of high density to porous sections of the material with a counter movement of lattice vacancies from high to low vacancy concentration areas. There are two types of diffusion that may occur; surface diffusion and volume diffusion. The smallest activation energy required for any of the sintering mechanisms is that required by surface diffusion, which occurs to some extent in all sintering processes. Surface diffusion, however, is only important during the initial stages of sintering because substantial densification cannot occur by this mechanism. For materials that sinter by diffusional mechanisms, surface diffusion is of great importance and is the cause of the initial adhesion between particles. It is then followed by volume diffusion which causes the densification.

The diffusion mechanism is produced by the motion of charged atoms or ions from their place in the lattice structure to an adjacent position, and so forth. Entire lattice planes do not shift during sintering by diffusion, which is the main difference between it and viscous flow sintering or sintering in the presence of a liquid phase.

Consider two isolated spherical particles touching one another. In order to decrease their surface energy, the two particles have a tendency to coalesce, forming one larger particle. It has been found that, when these two particles just touch one another, the concentration of vacancies is greater in the region of contact than throughout the remainder of the particle. This is because the concentration of lattice vacancies is always greater under a concave surface than under a convex one. The two particles touching form a concave surface at the bond zone. Thus material will begin to migrate toward the bond zone or, if you wish, lattice vacancies will begin to migrate from the bond zone.

Diffusional mechanisms of sintering are typical of crystalline and metallic materials.

If a diffusional mechanism is causing sintering, the material will decrease in size as indicated by the equation below.* The change in length may be measured using a dilatometer. (The dilatometer is discussed in a later section.)

$$\frac{\Delta L}{L} = \frac{D a^3 \delta}{r^3 kT} t^{2/5}$$

where

$\frac{\Delta L}{L}$ = fractional shrinkage

D = diffusional coefficient

δ = surface tension

a = lattice parameter

r = grain radius

- k = Boltzman constant
T = absolute temperature
t = time of sintering

3.2 Material Transport by Viscous Flow

Material transport by viscous flow is due to the effect of surface tension. The surface tension varies with the curvature of the surface and causes material to be transported from convex to concave regions, concave regions being formed by the contact between particles.

Most polymeric, glassy and non-metallic materials sinter by a viscous flow mechanism. For the purpose of this report, it will be assumed that sintering in the presence of a liquid phase is by viscous flow.

Depending upon the radius of curvature and the surface tension of the material being considered, surface forces producing viscous flow can exceed the equivalent of several thousand pounds of negative hydrostatic pressure. In materials that tend to creep (i.e., that have permanent deformation due to loads applied below their yield stress) equivalent pressures of this magnitude will generally produce significant viscous flow. The rate of this viscous flow will be determined by the material's coefficient of viscosity.

On a microscopic scale, it is generally accepted that viscous flow occurs due to the movement of lattice planes, as opposed to the movement of single atoms during a diffusional mass transfer mechanism. Thus, the material transported and bond area growth will be much more rapid if the sintering takes place by viscous flow, rather than by diffusion. The ability of the material to

allow movement of complete lattice planes is characteristic of material that will sinter by viscous flow.

Since the major constituent making up many coal ashes is a glassy material, it is probable that coal ash in general will behave in a manner similar to glass at higher temperatures. In some proposed coal gasification operations the final product of the coal will be a glassy type slag. Coal ash in these regions will probably sinter, due to a viscous flow mechanism. However, at lower temperatures, since a major part of the ash is derived from metallic materials, one might expect a diffusional type of coal ash sintering. Hence, two different mechanisms might be important in coal ash sintering, the predominance of one of the mechanisms depending on the sintering conditions and the ash composition.

If a viscous flow mechanism is causing sintering, the material will form a bond zone at the rate indicated by the equation below[#]. In the initial stages of sintering, the bond area may be estimated using a dilatometry test.

$$\frac{x^2}{r} = \frac{3\gamma t}{2\eta}$$

where

- X = bond zone radius
- r = particle radius
- γ = surface energy per unit area
- η = coefficient of viscosity
- t = time of sintering

The self-diffusion in crystalline material is believed to occur through their ability of the individual atoms to "flow". Although this type of flow is not the same as in the viscous mechanism, the self-diffusion coefficient is related to the coefficient viscosity: #

$$\frac{1}{\eta} = \frac{Da^3}{kT}$$

η = coefficient of viscosity

D = diffusional coefficient

a = lattice parameter

k = Boltzman constant

T = absolute temperature

3.3 Material Transport by Vapor Transfer

The vapor pressure above a concave surface is lower than that above a plane surface by an amount that is inversely proportional to its radius of curvature. The rate at which material is transported by vapor transfer, evaporation and condensation, is expressed as a function of the difference of the equilibrium partial pressure above the surfaces.

Consider two spheres in contact. The equilibrium partial pressure above the concave neck at the bonding zone, is less than the equilibrium partial pressure above the convex surface of the sphere. This will cause material to be transported from the surface of the sphere to the bonding zone, increasing the strength and area of the bond.

Material transfer by vapor transport is not considered to be of any significance, except for ultra fine particle sintering at low temperatures. For particles larger than one micron, the vapor transport rate can be considered negligible. Thus, it is likely that this mechanism plays no part in the agglomeration of coal ash in a fluid bed. However, if volatile phases are possible, intermediaries of the ash material during the combustion or gasification of the coal then vapor transport may be possible and should be considered.

If a vapor transport mechanism is causing sintering, the material will form a bond zone at the rate indicated by the following equation# In the initial stage of sintering, growth of the bond zone may be estimated using a dilatometer.

$$\frac{X^3}{r} = \frac{3\pi M \gamma (M/2\pi RT)^{\frac{1}{2}}}{\rho^2 RT} P t$$

where

- X = bond zone radius
- r = particle radius
- M = molecular weight
- γ = surface energy per unit area
- R = universal gas constant
- T = absolute temperature
- ρ = density
- P = vapor pressure above a flat surface
- t = time of sintering

3.4 Summary of the Sintering Rate Equations

Neck Growth

- $x \propto t^{1/2}$ for mass transport by viscous flow
 $x \propto t^{1/3}$ for mass transport by vapor transport
 $x \propto t^{1/5}$ for mass transport by volume diffusion with a spherical surface
 $x \propto t^{1/7}$ for mass transport by surface diffusion

Densification

- $\frac{\Delta L}{L} \propto t^2$ for mass transport by viscous flow without deformation of the particles
 $\frac{\Delta L}{L} \propto t$ for mass transport by viscous flow with deformation of the particles
 $\frac{\Delta L}{L} \propto t^{2/5}$ for mass transport by volume diffusion with a curved interparticle grain

3.5 Stages of Sintering

There are three stages of sintering that can be distinguished during the complete sintering process. These overlap but may be easily distinguished from one another. The initial stage is caused by the occurrence of stresses caused by the contact of particles along a boundary. These forces cause the particles to adhere and some early neck growth begins. If only this stage of sintering is reached, the particles are easily broken apart.

The second stage of sintering consists of densification in the bond zone area. Material is transported to

this zone as the area of the bonding increases and the particle centers begin to move together. At this point, the particles cannot be easily broken apart at the boundary.

The third and last stage of sintering is that of continued and complete densification of the two particles into one.

As we will see later, defluidization is caused by the adhesion produced between particles during the initial stage. The defluidization of a bed of fluidized particles will take place when the bonds, caused by sintering, cannot be broken apart by the kinetic motion of particles in the bed.

* J. D. Watt, BCURA Industrial Laboratories, Leatherhead, England, "The Physical and Chemical Behavior of the Mineral Matter in Coal Under Conditions Met in Combustion Plant", (August 1969).

M. Herman, "An Investigation of the Early Stages of Sintering", University of Pennsylvania, Ph.D., 1965.

4. Behavior of Coal Ash at High Temperatures

It is necessary to know the effects of exposure to high temperatures on coal ashes. This information, together with their fluidization characteristics, will enable us to more clearly understand what is happening when a bed, made primarily of coal ash, defluidizes.

The important factor to consider when looking at coal ash, is that this mineral matter is not homogeneous and depends upon the origin of the coal and the conditions under which it is combusted. When the ash is exposed to higher temperatures, the constituents present will tend to react with one another quite differently from the way they might behave had the pure material undergone similar treatment.

The original structure of the ash is in the form of a heterogeneous solid mixture of inorganic oxides and minerals. When this ash is heated it will eventually become molten, turning into an almost homogeneous liquid phase. This takes place continuously although several physicochemically different processes take place during this process. The first step in the formation of the molten ash is the formation of a melt from a binary mixture of two of the constituents present in the ash. These binary mixtures, in some cases, will experience much lower melting temperatures than the individual constituents from which they were formed. It should be remembered that the formation of these binary mixtures was by solid state diffusion, concentration gradient being the driving force. This initial melting or softening of the coal ash, may be sufficient to cause ash agglomeration or defluidization if sufficient sintering can occur. Although sintering is usually considered a physical, as opposed to physicochemical mechanism, this melting could cause sin-

tering to take place by viscous flow in the presence of a liquid phase.

The lowest temperature at which any of the products of the binary reactions will melt is the eutectic temperature. Once some melting has occurred, the liquid phase will act as a medium for further reaction. Much greater reaction rates will be encountered in the liquid phase due to the increased rates of diffusion above that in the solid state.

At slightly higher temperatures the amount of material in the liquid phase will increase and the components still in the solid phase will disappear, leaving a homogeneous liquid melt. When this melt is cooled the material may remain homogeneous forming a glassy like material, or the crystals may separate giving rise to a more heterogeneous material. This will depend upon the heating and cooling rates encountered. Thus, the viscous nature of the ash will depend not only on its constituents, but also on the manner in which they are treated. This is of significance because the defluidization experiments that were conducted used spent ash that was produced by burning coal. Depending upon the exact process used, the ash used in the defluidization experiments would be quite different from the ash produced during combustion or gasification of a freshly fed coal. This fact aside, it is believed that the experiments conducted tend to show the generally expected behavior of materials in the region of temperature where defluidization difficulties may appear. In addition, the data presented is intended only as an example of this behavior and any extrapolation to other systems should be on a qualitative basis only.

In addition to reactions that take place at the individual constituent or eutectic temperature, mixtures of solids can often react at temperatures substan-

tially lower where no portion of the solid can become molten. The reaction rates, although much less than if in the liquid phase, may be appreciable. These solid phase or solid state reactions occur by the migration of charged atoms or ions from one particle to another in contact with it. This reaction continues at the surface of the particles, causing a product layer to form between them, increasing in thickness as the reaction proceeds.

The mass transfer mechanism discussed above is one of solid state mass diffusion. By this same mechanism material may be transported toward a bond zone during sintering, causing the bond area to grow and the bond to become stronger. It seems possible that coal ash agglomeration may occur by different mechanisms depending on the temperature being considered.

Reactions in the solid state are due to migration of charged atoms through the material to a point at which they may react. This migration is due to the existence of vacancies in the lattice structure of the reacting material that allow movement of charged atoms from one position to an adjacent one in the lattice structure.

It is interesting to stop here and note the difference between motion, or migration of atoms by solid state diffusion, and by viscous flow. In solid state diffusion, as described above, atoms move from one adjacent position to another. Often, in the sintering literature, this is discussed as a lattice vacancy migration from one position to an adjacent one. In viscous flow, an entire row of atoms might shift position in the lattice so that the vacancy moves from one side to the other rapidly. Movement of the entire lattice plane in the viscous flow mechanism is the key difference between

the two.

The rate of solid state diffusion is believed to become appreciable when the temperature is some constant fraction of the melting temperature, usually 0.5 to 0.7. The current study has shown that, while this may be so, it has no effect on the agglomerative tendencies of the materials studied. The "initial stickiness temperature", to be defined in a later section, was not found to be any specific fraction of the melting temperature.

Reactions of binary mixtures often found in coal ashes have been studied extensively. It is not the intent of this section, however, to expand on these specific reactions. A complete survey has been compiled by Watt (1969) from which much of the material in this section was obtained. Watt makes the observation that these many investigations of solid phase reactions of mixtures, that are also contained in coal ashes, contribute little to the solution of practical problems of ash behavior in the plant. In the case of the current study it should be clearly understood that no attempt should be made to extend the results to operating equipment without further testing. The purpose of this study is only to provide a clear and concise work on the current knowledge of the phenomena of defluidization, including experimental findings and general background material included to aid in more complete understanding of the phenomena. The usefulness of this work is of a more qualitative than quantitative nature and no attempt has been made to extend the results to systems not studied.

4.1 Determination of Coal Ash Sintering Temperatures

A mechanism for ash agglomeration has been described by Harvey and Masters (1974). As the coal undergoes gasification, clay materials, quartz and pyrite grains begin to fuse along microscopic planes within the coal particles. The molten matter begins to move along these planes to the surface of the particles where it forms molten beads. These join with adjacent beads to form larger beads of molten ash. Molten beads come into contact as particle collision occurs in the fluidized bed, causing additional growth and reduction in number. As the agglomerates pass through the fluid bed, they continue to adhere to one another, forming multiglobular agglomerates.

According to the temperature, atmosphere, time of heating and composition of the coal, the final products of combustion may be ash, a sintered or fused clinker, or a slag (Watt 1969). Since the function of the plant and removal of ash matter will depend upon the physical operation and composition of the coal, there is practical justification for looking into the agglomerating tendencies of ash-like materials.

One of the processes involved in the agglomeration and collection of ash in the Ignifluid, is the physical agglomeration, sintering of particles of minerals and oxides at temperatures well below their softening points. The purpose of studying this phenomenon would be to predict whether a particular coal ash would tend to agglomerate under specified conditions in a plant. One of the major problems in plants fired by mechanical stokers has been the adhesion of the ash to the grate. The ash would melt and stick to the bars and other parts of

the boiler. This would often lead to complete plant shutdown for cleaning.

Since the sintering of the ash is an essential part of the process, it would be desirable to develop a laboratory test that could be related reliably to the agglomerating behavior of the ash under the conditions found in the plant. A large number of tests to determine the relative ash fusibility are available. Most early methods have used the "Seeger cone test" in which a sample of ash was formed into a pyramid with an acute angle and then heated under controlled conditions, until the cone underwent a predetermined change in shape. This test was refined to the U. S. Bureau of Mines and later led to the development of an A.S.T.M. test method (ASTM-D1857-61T).

Ash fusion temperatures are not reliable indicators of how a particular ash behaves under boiler conditions. A more reliable test method was necessary to establish, in advance, the potential ash-fouling tendency of a given coal. Barnhart and Williams (1956) have developed a sintering test that has been used to classify coals, and to determine their fouling characteristics. This sintering test consists of collecting several ash samples from the boiler, screening the material and making small pellets. These pellets are placed in a furnace and heated to the sintering temperature. After cooling, the sintered pellets are faced and their compressive strength is related to the fouling tendency of the ash.

An improved sintering test, using a dilatometer to measure the deformation of the compacted ash pellets as the temperature is increased, is being developed at the Babcock and Wilcox Alliance Research Center, Alliance, Ohio (S. Vecci 1973).

5. EXPERIMENTAL APPARATUS AND METHOD

The proposed research plan was to determine high temperature defluidization limits for several types of particles. In order to do this it was necessary to construct equipment that would provide hot fluidizing gas to the bed.

5.1 Experimental Equipment

Fluidizing gases are heated in one of two ways. The first involves the use of standard electrical heating elements, or "glow-bars" (Carborundum Co.). A current is passed through an arrangement of these bars and heat may be transferred by radiation from the heated bars. The fluidizing gases flow through a pipe around which these heating elements are placed. By this method the gases receive the heat indirectly.

Figure II shows the indirectly heated equipment. Air enters the bottom of the furnace and flows through a packed column used to increase heat transfer, and then to the fluidized bed. A perforated distributor plate is used to support the bed and is located well above the heating furnace. The reason for locating the bed so far above the furnace is to reduce the effects of localized hot spots. If the bed were located in the furnace area, it was found that the tube walls around the bed were much hotter than the fluidizing gas and, therefore, melting of the bed material at the wall occurred well before defluidization caused by the increase in temperature of the fluidizing gases. With the bed out of the furnace it is found that the walls of the bed are actually lower in temperature than the bed fluidizing gases.

This equipment is limited in that it

cannot reach temperatures beyond about 400F, although it has proved to be very easy to control. The indirectly heated equipment was used for all studies of polymeric materials at relatively low temperature.

The second method for heating the bed involves direct heating of the gases. A combustible gas, such as methane, may be mixed with the fluidizing air and then combusted, raising the temperature of the gases. The combustion gases can then be used to fluidize the bed. This second method has the advantage of allowing the type of atmosphere being used to be varied by controlling the air/gas ratio.

Figure III shows the directly heated equipment. Details of the combustion section are shown in Figure IV. A combustible gas and air are mixed in a venturi mixer and then fed into the combustion chamber. There is a solenoid safety valve on the gas inlet line to close the gas feed if the flame is extinguished. An excess air line is available to control the type of atmosphere desired.

The combustion is initiated by passing a current through a small coil of wire in the combustion zone. Gas is allowed to enter through a pilot supply until the combustion is proceeding normally, at which time, the solenoid control can be opened. The combustion takes place in a ceramic tube, surrounded by high temperature insulation. The entire combustion section is enclosed in stainless steel.

The fluidized bed is supported, using a conical distributor that was designed to allow the gases to enter at 120° to the direction of the gases in the bed. This design eliminated all downflow of fine material which was found to be a problem with the perforated plate type distributor.

A two inch diameter fused quartz tube is used as the bed wall. This allows for visual observation of the defluidization. This directly heated reactor was used for obtaining results for the copper and glass particles, and for mixtures of glass and silicon carbide.

A third experimental set-up was developed to allow experiments at even higher temperatures than could be obtained in the directly heated fluidized bed. It was also what could be termed a directly heated bed, except that the combustion of the methane and air mixture would occur above the distributor plate and in the fluidized bed itself. The diameter of the bed was six inches.

Several different distributor types were evaluated for use with this six inch bed. The major use of this bed was to perform "shallow bed" work, so that use of a conical distributor, as in the original directly fired equipment, would not be possible. In addition, relatively fine material was to be treated so that a perforated plate would tend not to support the bed as in the indirectly heated reactor. It was decided to use, either a porous disc, or a sintered metal plate.

At first, a sintered plate made of stainless steel was tried and seemed to perform satisfactorily at lower temperatures (below 2000°F). But at higher temperatures, it buckled severely and lost porosity. Thus, the sintered metal plate was found to be unsatisfactory for use in this work.

Two types of porous discs were found to be satisfactory at higher temperatures, although cracking was observed due to the rapid cycling of temperature during operation. One of them was a simple filter disc, and the other was made from material similar to a grinding wheel.

Specifications of these discs were that the porosity was to be such that a pressure drop of approximately one psi would be produced for an ambient flow velocity of ten feet per second.

The six inch bed was used for all the experimental work done on coal ashes. The instrumentation used, for all three experimental units, was identical. A probe was inserted into the fluidized bed from above which contained a thermocouple, pressure probe and locating pin. The purpose of the locating pin was to leave the temperature and pressure probes located in the identical spot for each run.

A type K exposed junction type thermocouple was used to measure the bed temperature. The pressure probe, which measured the pressure drop through the bed, was made from a standard 1/8 inch diameter stainless steel tube. Temperature in the bed, and pressure drop through the bed, were measured using digital indicators, and were plotted using a strip-chart recorder.

5.2 Sample Preparation

Sample materials used in the defluidization experiments were obtained from many sources and required varying amounts of preparation before use.

By far, the least preparation was necessary for the polymeric materials. These were available in an extruded pellet-type form of differing shape (the shape depending on the die used during the extrusion process). The only preparation necessary was to break apart any attached particles, so that the starter bed would contain only single particles.

The glass material also required little preparation. It was obtained pre-sieved to size and ready to use. Some samples were re-sieved to confirm the size as a check on the material. All the glass mat-

erial was obtained as almost true spheres.

The copper particles required substantial preparation in that it was necessary to sieve the material to the sizes desired before any experimental work could be done.

Coal ash samples required the greatest amount of sample preparation. Before the ash sample could be sieved to the desired size, it was necessary to remove the moisture from it as the ashes were received "wet". The ash material was dried in a vacuum oven at a temperature of approximately 300^oF and a vacuum of 29 inches of water. The coal ash remained in the oven for a period of several hours. After the ash was dried it could be sieved to the desired sizes.

The preparation of the coal ash proved to be very time consuming, thus limiting the number of ashes that could be studied in a reasonable period of time.

5.3 Determination of Defluidization

Before the initiation of this work there seemed to be no established method whereby the condition of the bed, with respect to defluidization, could be determined without visual observation. As a result of this study, it has been found that the point of defluidization may be determined by observing both the temperature in the bed and the pressure drop through the bed.

When the bed defluidizes the material will clump together on the gas distributor, blocking the flow of the fluidizing gas. Since the forces holding the individual particles together are small, compared to the pressure forces of the flowing gases, "rat holes" or

"channels" will be blown through the bed. The pressure drop through the bed with rat holes is substantially less than that of the original fluidized bed. Examination of beds, after experiments were conducted, clearly showed these channels blown through the bed. Thus, the bed defluidization is indicated by a sudden decrease in the pressure drop through the bed, as shown in Figure V.

In addition, when the material in the bed defluidizes, it falls down around the thermocouple's open junction causing an increase in the temperature to be indicated. This increase is usually small, and the use of it, to determine defluidization, in most cases seems limited. The relative magnitude of the increase in temperature, as compared to the pressure drop through the bed decrease, is illustrated in Figure V.

Visual observation of defluidization was possible when using the directly heated bed or the high temperature six inch bed. This visual observation was not necessary since a test had been established and was only used to check on the bed activity and reliability of the instrumentation from time to time.

In all cases the visual observation of defluidization was confirmed using the temperature in the bed and the pressure drop through the bed.

5.4 Determination of a "Sticky Temperature"

Each of the materials studied was found to have some temperature limit, at which it became "sticky" and began to self-adhere. The definition established for this temperature was such that, if a fluidized bed was being fluidized at just the minimum fluidization velocity and its temperature was raised, it would de-

fluidize when the temperature in the bed was equal to the "sticky temperature".

In order to establish some reproducible test to determine this temperature, the work of Dr. Vecchi (1973) at Babcock and Wilcox was followed. His findings showed that the "fouling" or "sintering" of coal ashes in boilers could be related to their sintering characteristics, established using a dilatometer. (A dilatometer is a device that simultaneously measures temperature and thermal expansion or compression of a sample.)

Dilatometry tests were performed on all the samples for which defluidization data had been obtained. These tests were performed by an outside laboratory because of the need for only a limited number of tests and the high purchase price of a dilatometer (Theta Industries).

The general nature of the dilatometry results were the same in all cases. As the sample temperature was raised from ambient, it exhibited thermal expansion. (The thermal expansion coefficient could have been determined using this initial part of the test). At some higher temperature the sample would no longer continue to increase in size, the effects of sintering balancing the effects of thermal expansion. Then, at some slightly higher temperature, the sample would begin to rapidly decrease in size due to a greatly increased rate of sintering, caused by the higher temperatures. The temperature at which the rate of sintering was found to increase greatly and cause a very rapid decrease in size of the sample, was found to correspond closely to the temperature at which a bed, at minimum fluidization would defluidize.

The sample prepared for the dilatometer was made to resemble the minimum fluidized state as closely as possible. The sample was held under minimum pushrod

pressure in a cylindrical sleeve with holes drilled to facilitate gas circulation (normal sample size was $\frac{1}{4}$ inch by $\frac{1}{2}$ inch long). The sample powder normally used in a dilatometer is cold pressed to hold it in position. It was felt that cold pressing would alter the results and would certainly not represent the condition in the bed at minimum fluidization.

The samples removed from the dilatometer appeared much like the samples taken from the beds after defluidization. The particles were loosely bonded together but could be easily broken apart.

5.5 Determination of Minimum Fluidization Velocities

Minimum fluidization velocities for the particle systems studied were calculated at the initial stickiness temperature, determined by dilatometry, using the following equation: **

$$\frac{\rho (\rho_s - \rho) d_p^3}{\mu^2} = 150 \frac{(1 - \epsilon_{mf}) U_{mf} d_p \rho}{\epsilon_{mf}^3 \mu} + \frac{1.75}{\epsilon_{mf}} \left[\frac{U_{mf} d_p \rho}{\mu} \right]^2$$

where:

- U_{mf} = minimum fluidization velocity
- g = acceleration due to gravity
- d_p = particle diameter
- ϵ_{mf} = bed voidage at incipient fluidization
- ρ = density of fluid
- ρ_s = density of solid
- μ = viscosity of fluid

For several systems at ambient conditions, minimum fluidization velocities calculated using this equation were found to be in agreement with those found experimentally, by measuring the pressure drop through the bed as the superficial velocity was increased and decreased:

<u>System</u>	<u>Experimental</u>	<u>Calculated</u>
Glass -14+16 U.S. Sieve	2.27 ft/sec	2.53 ft/sec
Glass -16+18 U.S. Sieve	2.16	1.93
Polyethylene Beads	2.12	2.19
Polypropylene Beads	2.63	2.76

** J. F. Richardson, "Incipient Fluidization and Particulate Systems", FLUIDIZATION, Academic Press, New York(1971).

5. 6

TEMPERATURE PROFILES

(Six inch shallow bed)

Experiments were conducted in order to determine the nature of the temperature profiles in the six inch shallow bed and how these profiles changed with time. The solids material used was -40+50 U.S. sieve sand, fluidized at slightly more than three times minimum fluidization. The feed to the six inch diameter bed was 350 cubic centimeters. Horizontal profiles were measured on the distributor and at one inch above it. Vertical profiles were measured as a function of time at the center of the bed.

The horizontal profiles indicated that, at points far enough above the distributor, the temperature was almost uniform ($\pm 15^{\circ}\text{C}$) across the bed. From the vertical profiles this minimum height above the distributor appears to be a function of time, decreasing with time of operation. However, it was found to remain constant at about 0.25 inches after five minutes.

On the distributor the temperature was found to decrease, as the thermocouple was moved from the center of the bed. This was expected since, it was assumed that large quantities of heat would be lost at the sides and the thermal mixing advantages of fluid beds would be minimal in the "virtually dead corners" of the bed. Slight variations to these profiles were found when the distributor was changed. This was probably due to possible non-uniformity of the distributor.

Vertical profiles were taken at several times. It was found that temperature variations of $\pm 30^{\circ}\text{C}$ or more were experienced vertically through the bed. The largest gradient occurred at the very bottom of the bed.

The distributor surface was obviously the "coldest" part of the bed and the large gradient found occurred the first quarter inch above it. Above this initial gradient the variation in temperature was found not to exceed $\pm 10^{\circ}\text{C}$. Temperature decreased rapidly at heights just above the bed where little elutriation occurred. The position of maximum temperature was found to fall with time. This was due to the fact that, when the bed was started the flame was above it, and only after the fluidized particles became hot, due to their passage at the bed's top surface, would the bed become hot enough to support combustion of the fluidizing gases in the bed. This lowering of the "combustion" point down through the bed, is in fact indicated by the change in position of the maximum temperature.

These temperature measurements were made using an exposed junction type thermocouple. Additional measurements were made using a shielded thermocouple and this indicated lower temperatures. Subsequent tests were made and it became evident that the shielded thermocouple would always give lower readings than the exposed junction type. This result was attributed to the fact that heat was transmitted through the shield and out of the bed, the effect being quite evident due to the small height of the shallow bed, as compared to the diameter of the shielded thermocouple.

It was decided to make all temperature measurements during defluidization at the center of the bed, since this was found to be the hottest region. In addition, since there were no large thermal gradients above the initial bottom one-quarter inch of the bed, the measurements would be made above this point. For all the defluidization experiments, the exposed junction thermocouple was placed approximately three-eighths inch above the

distributor.

Figures VIa,b andc are typical of the temperature profiles found for the six inch shallow bed during this study.

6.

EXPERIMENTAL RESULTS

A primary hope of this work was to demonstrate that the defluidization of beds of sticky particles is a well ordered phenomenon obeying precise rules. Many different particle systems were studied, including metallic, polymeric and glassy materials, which would exhibit different mechanisms of sintering. In addition, defluidization results were obtained for several different coal ashes. In all cases, results were found to conform with the previously expected behavior shown in figure I, where as the temperature was increased the fluidization velocity had to be increased to prevent defluidization from occurring.

The experimental results are illustrated in figures VII through XXXV. The defluidization results are presented as an excess velocity necessary to maintain a fluidized condition at an excess temperature (the excess velocity is that above the minimum fluidization velocity, and the excess temperature is that above the "initial sticky temperature"). The experimental data are given in each figure along with the line which best fits them. The data is also presented in tabulated form in appendix II. The equation of the curves, along with their regression coefficients are given in appendix IV.

Experiments were initiated using several sizes of copper particles. These particles were chosen because they would exhibit sintering by a surface or volume diffusion mechanism. In addition, since the copper is a "pure" inorganic substance, it exhibits a sharp and predictable melting point. Although pure copper particles were used, all of the experiments were conducted in an oxidizing atmosphere. This produced an oxide coating on the particles,

causing the bonding or sintering to take place between the oxide coatings rather than between the copper core.

The coating the copper particles received was believed to be of cupric oxide, which has a melting point of 1879^oF. Since most of the defluidization results obtained were well below this temperature, it could be assumed that no melting of the particles, or of their coating, took place. This was confirmed by visual observation and photomicrographs (see section on Agglomerate Examination).

The defluidization limits for the copper particles are presented in figures VII through IX and the sintering studies in figure XXXI. The results of the sintering studies are typical for a powdered metallic substance, an initial increase in size due to thermal expansion at low temperatures, followed by a leveling off as the material begins to sinter and a reduction in size as the rate of sintering begins to increase substantially. Since the "initial sticky temperature" is defined as the point at which the rate of sintering begins to increase substantially, for the copper particles it was the maximum on the thermal expansion curve, just as the size of the sample began to decrease rapidly.

Using -16+20 U.S. Sieve copper powder, experiments were conducted to determine the effect of different heating rates on defluidization. Experimental times ranged from one half hour to eight hours. There was no apparent effect on the point of defluidization. In addition, experiments were made where the bed would be brought to a temperature about 50°F below that necessary to cause defluidization. Even after several hours of operation at this condition, the bed did not defluidize until the temperature was increased to that normally necessary to cause defluidization.

While performing the defluidization experiments on the copper powder, an interesting effect was discovered that might add to the understanding of the process discussed where various metallic oxides were reduced in a fluidized bed. If the bed were fluidized in an oxidizing atmosphere at a temperature well below that necessary for defluidization, and the atmosphere was then changed to reducing by greatly increasing the relative amount of methane gas to air being fed into the combustion chamber, the bed would defluidize immediately as the oxide coating on the particles was reduced. In addition, sintering studies were conducted on this copper powder under a reducing atmosphere and results

showed that the "initial sticky temperature" was significantly higher than that obtained for the same material under an oxidizing atmosphere. This was expected since the melting temperature of the reduced copper was approximately 100°F higher.

It is believed this unpredicted defluidization was caused by a sudden increase in the particle surface temperature which was not observed as an overall increase in temperature of the bed. As the oxide coating on the particles was reduced, large quantities of heat were released on the particle surfaces causing some probable surface melting and adhesion of the particles. This operation was believed to occur rapidly enough so that an increase in the overall bed temperature would not be noticed. It was found that the agglomerates formed in this way were much more strongly bonded together than were those produced under a continuous oxidizing atmosphere experiment.

Experiments were conducted using several different polymers; polyethylene, polypropylene, lexan and dacron. All of the materials exhibited sintering by viscous flow. The defluidization results are presented in figures X through XIV. The effect of increasing bed height is illustrated for polyethylene beads in figure XXIX. The results of sintering tests on the polyethylene and polypropylene beads in figure XXXII.

The sintering test results for the other polymeric materials were very similar to those obtained for polyethylene and polypropylene. In most cases they would undergo a very rapid decrease in size over a narrow temperature range just at the initial sticky temperature. This made the determination of T_g much less difficult than it was for materials that showed little decrease in size (increase in sintering) over large temperature ranges.

The effect of bed depth on defluidization was ex-

pected. As the height of material in the bed was increased, at a constant fluidization velocity, the temperature necessary to defluidize the bed was found to decrease. It is believed this is due to decreased particle mixing and momentum, due to an increased tendency to slug in the bed, the slugging bed providing much less mixing as the length to diameter ratio of the bed is increased.

Before experiments were conducted on coal ash, it was desired to conduct experiments on materials that would behave in a similar way at lower temperatures. For this reason silicate glass spheres were used during experiments conducted in the two inch directly heated bed. The results of these experiments are presented in figures XV and XVI. The effect of bed depth on glass defluidization is presented in figure XXX.

The results of the sintering studies performed on the glass spheres are given in figure XXXIII. The solid curves presented represent the general trend of several thermal expansion tests on each size of glass. Many of the tests indicated a region in which there was no change in length over a long temperature range, and then a sudden decrease. It was found that this sudden decrease always occurred at the same temperature for the same size of glass, the initial stickiness temperature.

The type of result described here, the extended horizontal maxima, or plateau, is illustrated by the broken line in figure XXXIII. This phenomena did not affect the results of the sintering test since the temperature at which the rate of sintering would greatly increase was the same in all cases, and a consistent initial stickiness temperature was easily obtained.

Defluidization results were obtained for three different coal ashes. For each coal ash, four sizes were studied. Compositions of these coal ashes are presented in appendix III. The results of this work are presented in figures

XVII through XXVIII. The results obtained are similar to those of the materials that had been studied previously.

It is interesting to note the behavior of the particles of ash supplied by American Electric Power (AEP) as they underwent defluidization. This ash was produced in a pulverized fuel fired dry bottom boiler. Microscopic examination of the particles, before being used for the defluidization experiment, showed them to be made up of many finer size particles so that the feed material to the bed were in fact agglomerates. The bond zones between these individual fines was easily seen. The particles were examined again after they were defluidized. At the second examination it was difficult to see that the original particles were made from fines. It seemed as though material had diffused toward the bond zone regions to obscure them, this diffusion being due to the tendency of the original particle to decrease its surface area and its porosity. Two simultaneous sintering operations had obviously occurred. The feed particles had loosely bonded together to cause the bed to defluidize, and the individual particles had undergone the final stages of sintering, where voids were removed between the fines.

The ash supplied by the Institute of Gas Technology (IGT) was atypical in that it contained close to 15% carbon. Once the bed reached a temperature of about 1200F, it was not necessary to supply methane to maintain the temperature increase. Since the flow rates were predetermined, it was almost impossible to control the temperature once the carbon started to "burn off".

The third ash used was supplied by Commonwealth Edison of Chicago from a pulverized fuel fired dry bottom boiler. The results for the defluidization tests on the Commonwealth Edison (CE) Ash were quite good except

for the smallest size, -40+50 U.S. Sieve, illustrated in Figure XXVIII. A large error in the experimentally determined initial stickiness temperature was evident and defluidization at incipient fluidization conditions occurred several hundred degrees below T_s . Comparison of T_s for all the CE coal ashes showed that, while values in the range of 1300°F were found for all except for the smallest size, and were consistent with the defluidization results, a value of 1939°F was found for the -40+50 U.S. Sieve CE coal ash. This value is obviously in error and is the cause of the inconsistency of the data presented in Figure XXVIII.

Defluidization temperatures for coal ash, reported here, are well below what those familiar with coal ash characteristics and softening temperatures would predict. However, it has been reported (Barnhart and Williams, 1956) that bonds of appreciable strength are formed between particles of coal ash at temperatures as low as 1500°F. The results that can be obtained from the standard A.S.T.M. Ash Fusion Test provide little information useful in predicting the defluidization phenomena.

Defluidization results were also obtained for mixtures of silicon carbide and glass. The purpose of these experiments was to study the effect of mixing an inert material (one that would not defluidize at the temperatures of interest) with one that would exhibit the characteristic defluidization behavior. The results are illustrated in figure XXXIV. It was found that, at a constant velocity, there was no effect on defluidization temperature when the amount of silicon carbide was varied from zero to eighty percent by volume, although it did seem to take longer to defluidize as the amount of silicon carbide was increased. This would show that, once a

certain percentage of the material in the bed would become "sticky", the bed would eventually defluidize. If a greater percentage of the bed material became sticky, it would still defluidize at the same temperature but perhaps in a shorter period of time.

In looking at the results it becomes evident that, as a group, the coal ash defluidization data shows the greatest disagreement with the experimentally determined minimum stickiness temperature. This is due to the way in which the dilatometry tests were conducted and T_s was determined and was limited to the coal ash results.

Figure XXXV illustrates the typical result obtained for dilatometry tests on the coal ash samples. There was no initial region where thermal expansion would take place as was seen with all other materials studied. The coal ash samples were quite different from any of the other materials in that they were initially very porous. In addition, a weakly bonded ash agglomerate could be formed by cold pressing the material by hand. For this reason it is believed that, as the temperature was increased, the sample tended to fill its own voids and decrease intra-particle porosity rather than exhibit thermal expansion. This caused major problems in the determination of the initial stickiness temperature T_s .

In order to remain consistent with the previously defined test, for the initial stickiness temperature, the point at which the rate of sintering greatly increases must be found. There was considerable difficulty in choosing an appropriate T_s for most of the coal ash material, in that the material exhibited some sintering at even very low temperatures.

To stay consistent with the results from the other materials studied, the value of T_s was taken as in-

licated in Figure XXXV, where a "higher" sintering rate begins. This difficulty in determining T_s is believed to be the major source of error for the coal ash results.

It is recommended that considerable additional work be done on the evaluation of dilatometry for the determination of T_s . This would necessitate the purchase of a dilatometer to perform the many experiments that would be required.

Overall, the results obtained were consistent in that, in order to avoid defluidization, the fluidizing velocity had to be increased as the temperature was increased. (The nature of the agglomeration process is discussed in the section on High Speed Photography. Photographs and micrographs of the agglomerates are presented in the section on Agglomerate Examination).

7. DEFLUIDIZATION MODEL

A theoretical model, describing the defluidization phenomena, can only be developed from a thorough knowledge of all the parameters that influence the defluidization temperature and velocity. The purpose of the model presented here is only to describe the gross behavior of fluidized beds in the region of agglomeration and defluidization and to compare the data from the many systems studied. Development of a model, based on stochastic or probabilistic theory, is beyond the scope of the present study and would serve no useful purpose for data comparison.

From previous industrial applications the parameters of interest can easily be determined. It was found that, at a constant velocity, the rate of agglomeration would increase as the temperature was increased until the bed would defluidize at the so-called defluidization temperature. The rate of agglomeration increase seemed to be due to an increasing sintering rate caused by the increased temperature. The sintering of the bed particles caused them to behave as if they were coated with a sticky substance where, as the temperature was increased, the mass of sticky substance on a particle would also increase.

As the fluidizing velocity was increased, it was found that the bed had to be brought to higher temperatures in order to have it defluidize. Increasing the velocity seemed to be causing greater particle motion and momentum, thus causing greater collision and breakup of the agglomerates that were forming. Thus it seems that the rate of particle agglomeration, in a fluidized bed, varies inversely with the momentum of the particles in the bed.

The amount of particle agglomeration that takes place at a given temperature and velocity, will also depend

on the amount of surface area available for interparticle contact. It was reported that smaller particles tended to show a greater tendency to defluidize than larger ones. Thus the smaller particles provided a greater total particle surface area in the bed.

All these effects were again observed in obtaining the defluidization data presented here. The rate of agglomeration in fluidized beds, due to stickiness caused by increasing temperature (sintering), has been related to the above results (Langston & Stephens, 1960):

$$\text{Agglomeration Rate} \quad \alpha \quad \frac{\text{Stickiness x Surface Area}}{\text{Momentum}}$$

Simply stated, the rate of agglomeration in a fluidized bed is proportional to the stickiness and the total surface area available for contact and inversely proportional to the particle momentum.

The stickiness, surface area and momentum can be expressed as numerical values that will be functions of the predominant variable affecting them and can be related by suitable mathematical relationships developed from observations of the defluidization phenomena and the theory of sintering and fluidized particles. The interpretation of the various terms of this simple model will produce a simplified equation that will describe the defluidization results already obtained.

PARTICLE MOMENTUM

The presence of this term simply indicates that, as we increase the particle momentum in the fluidized bed,

they are less likely to become adhered to one another and, if they become attached and form an agglomerate, are more likely to collide with other particles and break apart. It seems probable that the momentum of the particle, also particle agitation, would increase with increasing fluidization velocity and be proportional to the excess velocity (i.e., velocity above the minimum fluidization velocity).

The units of momentum are mass times velocity. The mass of a particle depends upon its density and volume. Combining into mathematical terms:

$$\text{Momentum} = \text{Mass} \times \text{Velocity}$$

$$\text{Momentum} = \alpha' d_p^3 \rho_s (U - U_{mf}) \quad \frac{\text{lb}_m \text{ ft}}{\text{sec}}$$

Where: U = superficial fluidization velocity (ft/sec)

U_{mf} = minimum fluidization velocity (ft/sec)

ρ_s = particle density ($\text{lb}_m / \text{ft}^3$)

d_p = particle diameter (ft.)

α' = constant

PARTICLE SURFACE AREA

The surface area of a particle available for contact depends on its diameter:

$$\text{Surface Area} = \alpha'' d_p^2 \quad \text{ft}^2$$

where: α'' = constant

PARTICLE STICKINESS

The most difficult term to express mathematically is the stickiness term. However, if we say that almost no

stickiness is necessary to defluidize a bed at minimum fluidization conditions, we can assign this point a zero value and relate the stickiness to the increase of some property above this point. Since we are interested in stickiness caused by high or increasing temperature, we can assign this zero as the "minimum sticky temperature", T_s , and the amount of stickiness as a function of the excess temperature, that above the minimum sticky temperature, $T - T_s$.

In addition, this term must have units of $\text{lb}_m / \text{ft sec}^2$ due to the constraints on the units of particle momentum and surface area. This term should also have some relationship to a pressure necessary to initially hold or push the particles together before they sinter. The following expression satisfies all the above criteria:

$$\text{STICKINESS} = g_c \alpha'' \frac{T - T_s}{T_s} \frac{\text{lb}_m}{\text{ft sec}^2}$$

T = defluidization temperature ($^{\circ}\text{R}$)

T_s = initial stickiness temperature ($^{\circ}\text{R}$)

α'' = contact pressure term ($\text{lb}_f / \text{ft}^2$)

g_c = constant ($32.2 \frac{\text{ft lb}_m}{\text{lb}_f \text{ sec}^2}$)

This result seems obvious since it has already been established that higher temperatures cause greater particle stickiness due to an increased rate of sintering, the only new criterion being that a bed fluidized at the minimum conditions, will defluidize when the temperature reaches the minimum sticky temperature.

Substituting all the terms into the original

equation: -

$$\text{Agglomeration Rate} \propto \frac{g_c \alpha''' \frac{T - T_s}{T_s} \alpha'' d_p^2}{\alpha' d_p^3 \rho_s (U - U_{mf})} \text{ sec}^{-1}$$

combining constants and simplifying:

$$\text{Agglomeration Rate} \propto \left[\frac{g_c \alpha'' \alpha'''}{\alpha'} \right] \left[\frac{1}{d_p \rho_s T_s} \right] \left[\frac{T - T_s}{U - U_{mf}} \right]$$

As the bed temperature is increased, or the fluidization velocity decreased, the agglomeration rate will increase until defluidization occurs.

A "defluidization index", η , might be defined as the product of the last two terms of the above equation:

$$\eta = \frac{1}{d_p \rho_s T_s} \left[\frac{T - T_s}{U - U_{mf}} \right]$$

This index is based on the macroscopic properties, or variables, of defluidization that were measured during the present experimental program, and, at least, indicates some of the important parameters to be considered when dealing with fluidized beds at high temperatures where substantial agglomeration of the solids may occur.

Calculated values of the "defluidization index" are presented in the following tables. The data, however, do not indicate that defluidization occurs at any specific value of the index. Perhaps the functional forms assumed are incorrect or additional variables, reflecting differences in the materials used, must be incorporated in order to formulate an adequate model.

SYSTEM	$\frac{d_p}{\rho} \text{ (ft)}$	$\rho_s \text{ (lb}_m/\text{ft}^3)$	$T_s \text{ (}^\circ\text{R)}$	$\frac{U-R}{U-R_{mf}} \frac{\text{sec R}}{\text{ft}}$
Copper - 16+20 U.S. Sieve	.0033317	556	2110	33.33
Copper - 20+30 U.S. Sieve	.002356	556	2010	14.29
Copper - 40+50 U.S. Sieve	.0011762	556	1841	74.63
Polyethylene Beads	.008	59	704	1.138
Polyethylene Balls	.0104	60	720	2.168
Polypropylene Beads	.00991	56.7	749	5.68
Dacron Beads	.00651	86	641	3.7
Lexan Beads	.00839	75	775	2.14
Glass - 14+16 U.S. Sieve	.004265	188	1670	16.67
Glass - 16+18 U.S. Sieve	.003553	188	1660	142.85
Coal Ash(AEP)-16+20 U.S. Sieve	.0033317	155	2066	47.6
Coal Ash(AEP)-20+30 U.S. Sieve	.002356	155	1841	142.9
Coal Ash (AEP)-30+40 U.S. Sieve	.001665	155	2021	166.7
Coal Ash(AEP)-40+50 U.S. Sieve	.0011762	155	2066	136.99
Coal Ash(IGT)-16+20 U.S. Sieve	.0033317	90	1823	49.5
Coal Ash(IGT)-20+30 U.S. Sieve	.002356	90	1841	75.8
Coal Ash(IGT)-30+40 U.S. Sieve	.001665	90	1823	66.67
Coal Ash(IGT)-40+50 U.S. Sieve	.0011762	90	1895	40
Coal Ash(CE) -16+20 U.S. Sieve	.0033317	105	1751	51.55
Coal Ash(CE) -20+30 U.S. Sieve	.002356	105	1751	62.89
Coal Ash(CE) -30+40 U.S. Sieve	.001665	105	1841	83.33
Coal Ash(CE) -40+50 U.S. Sieve	.0011762	105	2399	121.95

<u>SYSTEM</u>	<u>$\eta \times 10^3 \text{ sec}^{-1}$</u>
Copper -16+20 U.S. Sieve	8.53
Copper -20+30 U.S. Sieve	5.43
Copper -40+50 U.S. Sieve	61.9
Polyethylene Beads	3.42
Polyethylene Balls	4.83
Polypropylene Beads	13.5
Dacron Beads	10.31
Lexan Beads	4.39
Glass -14+16 U.S. Sieve	12.4
Glass -16+18 U.S. Sieve	127.4
Coal Ash (AEP) -16+20 U.S. Sieve	44.6
Coal Ash (AEP) -20+30 U.S. Sieve	212.6
Coal Ash (AEP) -30+40 U.S. Sieve	319.6
Coal Ash (AEP) -40+50 U.S. Sieve	363.7
Coal Ash (IGT) -16+20 U.S. Sieve	90.6
Coal Ash (IGT) -20+30 U.S. Sieve	194.2
Coal Ash (IGT) -30+40 U.S. Sieve	244.1
Coal Ash (IGT) -40+50 U.S. Sieve	199.4
Coal Ash (CE) -16+20 U.S. Sieve	84.16
Coal Ash (CE) -20+30 U.S. Sieve	145.19
Coal Ash (CE) -30+40 U.S. Sieve	258.91
Coal Ash (CE) -40+50 U.S. Sieve	411.16

8. CONCLUSIONS

The results of this experimental program have shown that defluidization is a well ordered and reproducible phenomenon which is independent of the means by which the particle sintering occurs. It seems possible to extend the results obtained here to other systems of particles, although only on a qualitative basis, in order to predict their behavior at higher temperatures.

Defluidization has been shown to be a sharp phenomenon where the bed can be well fluidized one minute and dead the next. As the bed defluidizes, the particles become loosely stuck together and the fluidizing gas blows a hole through the mass of particles to escape. As the hole appears the pressure drop, through the bed, decreases dramatically. This behavior was used as an indication of the point of defluidization.

Agglomerate examination indicated that in general the particles, although stuck together, maintained their original shapes after defluidization. This indicated that neither melting nor substantial softening had taken place. In general the forces, holding the particles together, were found to be very weak. Rolling an agglomerate of copper particles between two fingers results in large numbers of particles breaking loose and separating from the parent agglomerate. This accounts for the ease with which a bed, that has been defluidized, can be refluidized if the velocity is increased.

The particles in the polymer and glass agglomerates were bonded together more securely than the copper agglomerates, but could still be readily broken apart by hand.

For any bed there is a temperature, T_s' , defined by the intersection of the high temperature limit and the minimum fluidization velocity line. The significance of this temperature is that it is the maximum value for which the traditionally accepted minimum fluidization velocity separates non-fluidized from fluidized beds. For any temperature above T_s' the minimum fluidization velocity would be the high temperature defluidization limit.

The traditional minimum fluidization velocity represents a balance of drag, buoyancy and gravity forces acting on a particle in a large system of particles. Once the bed is above the "initial sticky temperature" T_s , at least two other major forces must be included in this balance, the kinetic energy forces due to the motion of the particles and the adhesive forces due to the sintering phenomenon. Therefore, the new high temperature limit, or high temperature minimum fluidization velocity curves represent the balance between drag, buoyancy, gravity, kinetic energy and sintering.

Analysis of the defluidization phenomenon by high speed photography showed that, in fact, there were two competing processes occurring in an agglomerating bed. First there was the formation of agglomerates of up to several particles, due to sintering at a temperature just below the defluidization point. Then these agglomerates collide and are usually broken apart as long as the bed

temperature is below the high temperature defluidization limit. Once the bed is above this limit, the rate of particle agglomeration greatly exceeds that of break-up and the bed will defluidize.

It is interesting to note that, since the initial stickiness temperature will cause defluidization at the minimum fluidization velocity, it is likely that for all beds operating above this temperature some particle agglomeration does occur. This may not be obvious because the bed may be fluidized at such a high velocity as to break apart these agglomerates almost as soon as they are formed. However, if an agglomerating bed operation is desired, it seems obvious that the process must be run at a temperature above the minimum sticky temperature T_s . Thus, a minimum temperature of operation for all agglomerating bed processes has been established. Once a temperature of operation has been chosen, the amount of particle agglomeration that will occur will depend on the fluidization velocity. Higher velocities will produce less agglomeration, while lower velocities will produce more.

The model that was developed illustrates the effects of the parameters of fluidization and sintering on defluidization. It was stated that the rate of agglomeration was proportional to the relative stickiness or adhesive force of the particles and the total particle surface area available for contact, and inversely proportional to the particle momentum. The stickiness was expressed as a function of the excess temperature above the minimum stickiness temperature, which was assigned a reference value of zero stickiness. The surface area available for interparticle contact was simply a function

of the particle diameter. The particle momentum was expressed as a function of, the particle diameter, density and the excess velocity above the minimum fluidization velocity. It should be remembered that, according to the two phase theory of fluidization, all gas above that necessary to produce minimum fluidization will pass through the bed as bubbles. Since the particle momentum should be proportional to the amount of bubbling in the bed, it seems obvious that it should be proportional to the excess velocity.

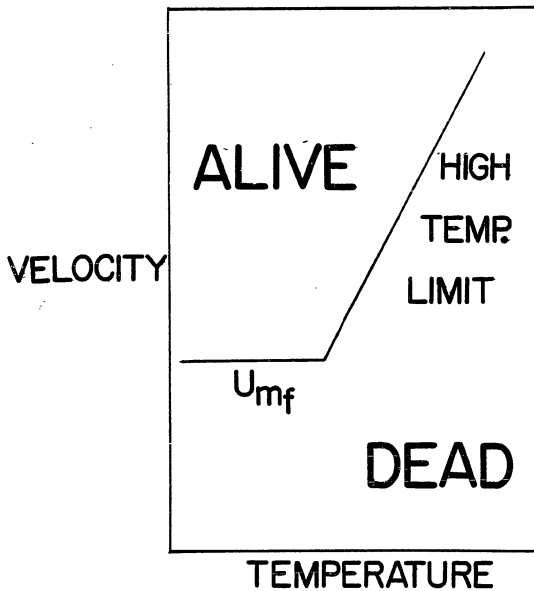
It should be remembered that this work was carried out with particle systems of a narrow size range, and extension to beds having a large particle size range is questionable.

For commercial or pilot scale work, the question arises as to how to determine the intersection temperature of the minimum fluidization curve with the high temperature limit. Two possible methods might be considered: one using dilatometry, the other using a small fluidized bed in which several defluidization experiments are performed to establish the high temperature defluidization limit. A comparison of these two methods from data in this work is made in the following table and in Figure XXXVI. Here T_s is the initial stickiness temperature, from dilatometry, and T_s' is the intersection temperature of the minimum fluidization velocity and the least squares line through the defluidization data.

Dilatometry does not appear to be wholly reliable for this purpose. One reason may be that the loading of the sample in dilatometry is arbitrary and does not correspond to the forces present in a fluidized bed. Ultimately, the testing of materials in a small fluidized bed may prove to be the more reliable and convenient method for establishing the start of the high temperature limit.

<u>SYSTEM</u>	<u>T_S(^OR)</u>	<u>T_S(^OR)</u>
Copper - 16+20 U.S. Sieve	2110	2110
Copper - 20+30 U.S. Sieve	2010	2148
Copper - 40+50 U.S. Sieve	1841	1776
Polyethylene Beads	704	704
Polyethylene Balls	720	717
Polypropylene Beads	749	741
Dacron Beads	641	641
Lexan Beads	775	779
Glass - 14+16 U.S. Sieve	1670	1735
Glass - 16+18 U.S. Sieve	1660	1744
Coal Ash(AEP) -16+20 U.S. Sieve	2066	1926
Coal Ash(AEP) -20+30 U.S. Sieve	1841	1489
Coal Ash(AEP) -30+40 U.S. Sieve	2021	2081
Coal Ash(AEP) -40+50 U.S. Sieve	2066	2057
Coal Ash(IGT) -16+20 U.S. Sieve	1823	1848
Coal Ash(IGT) -20+30 U.S. Sieve	1841	1961
Coal Ash(IGT) -30+40 U.S. Sieve	1823	2136
Coal Ash(IGT) -40+50 U.S. Sieve	1895	1899
Coal Ash(CE) -16+20 U.S. Sieve	1751	1646
Coal Ash(CE) -20+30 U.S. Sieve	1751	1767
Coal Ash(CE) -30+40 U.S. Sieve	1841	1873
Coal Ash(CE) -40+50 U.S. Sieve	2399	1924

APPENDIX I: FIGURES



F.1

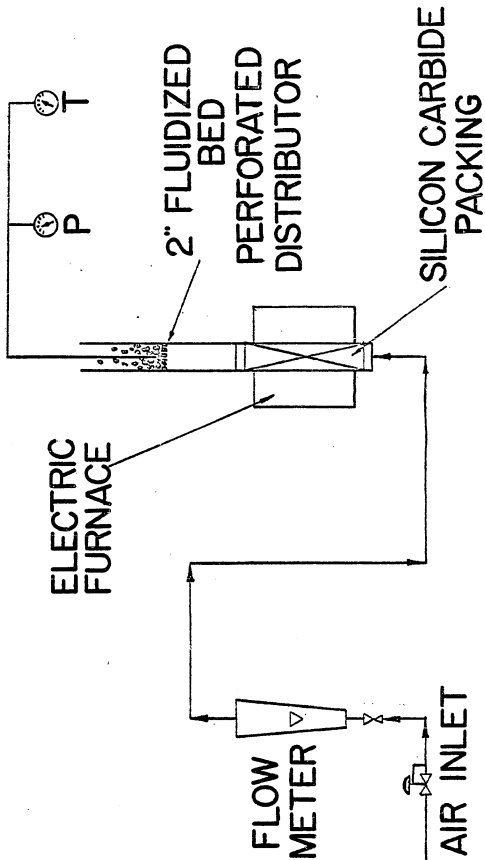


Figure II. Indirectly Heated Equipment

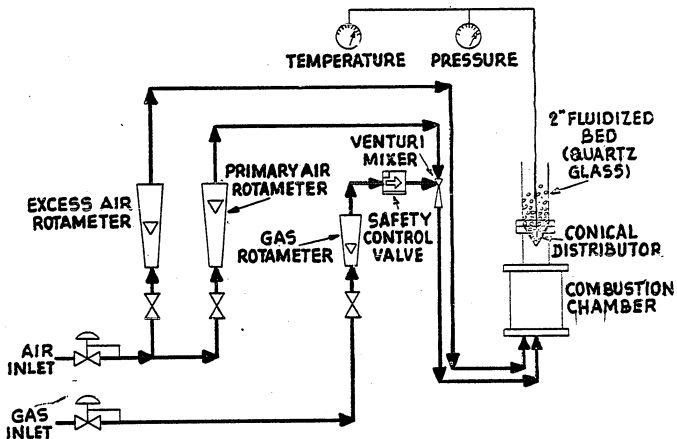


Figure III. Apparatus for Studying Defluidization Limits of a Directly Heated Fluidized Bed.

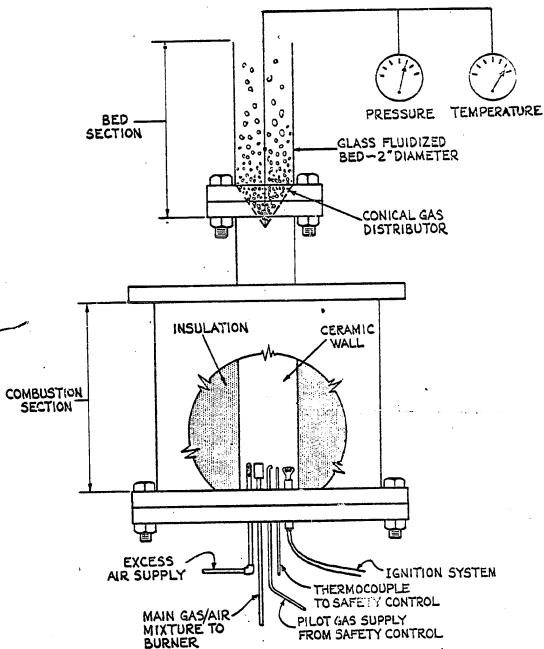


Figure IV. Details of Apparatus for Studying Defluidization Limits of a Directly Heated Fluidized Bed.

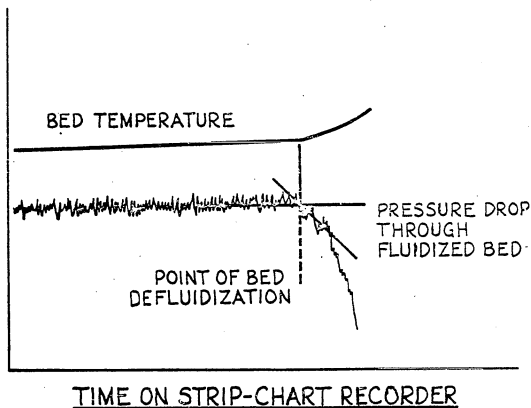
DEFLUIDIZATION DATA

Figure V. Plot of Bed Pressure Drop and Temperature vs. Time for a Defluidization Experiment.

HORIZONTAL PROFILES

Figure VIa:
ONE INCH ABOVE DISTRIBUTOR
TWENTY MINUTES AFTER START-UP

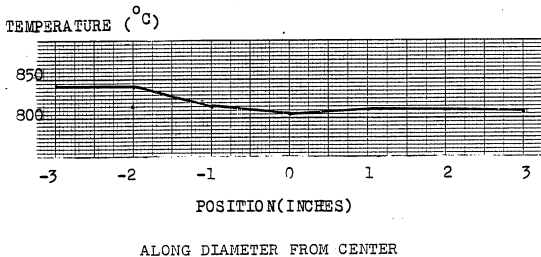


Figure VIb:
ON DISTRIBUTOR
TWENTY MINUTES AFTER START-UP

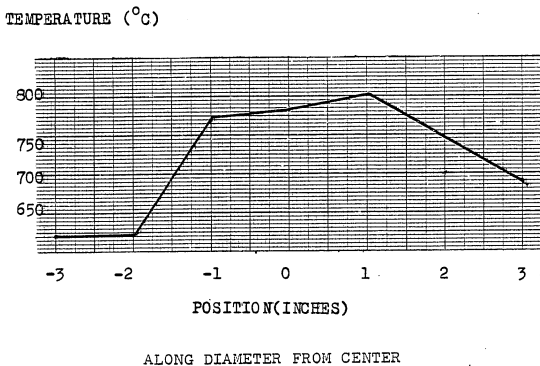
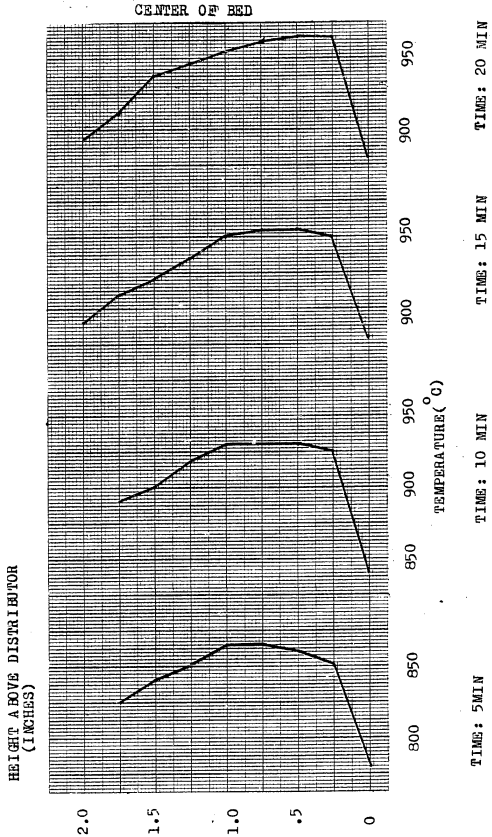
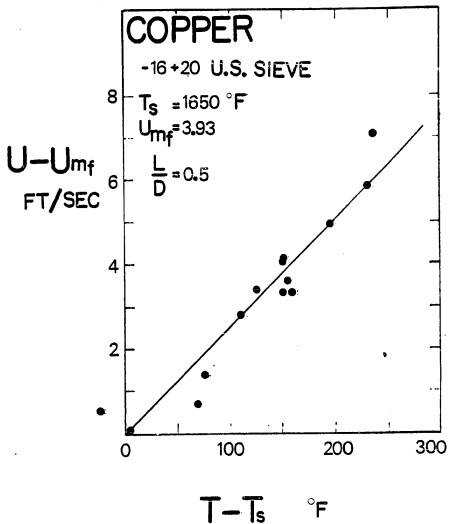
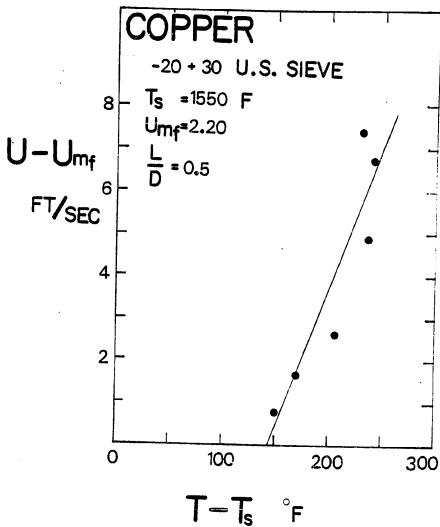


Figure VIc. VERTICAL PROFILES

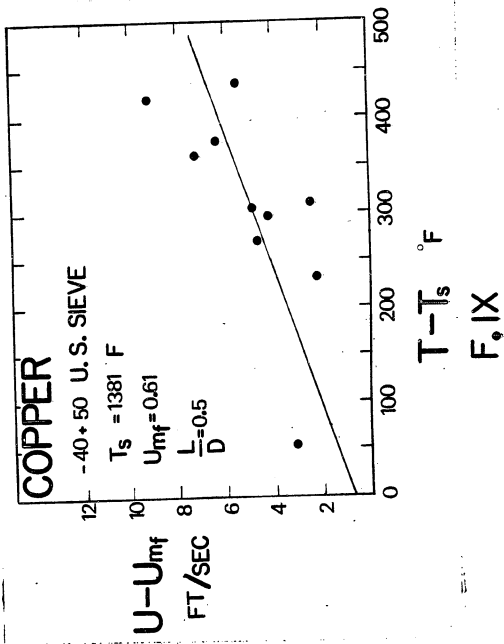


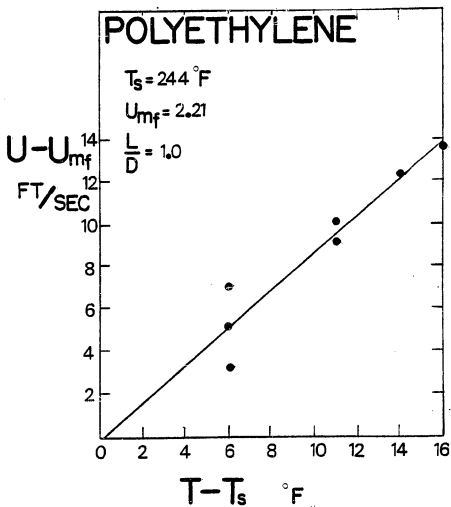


F. VII

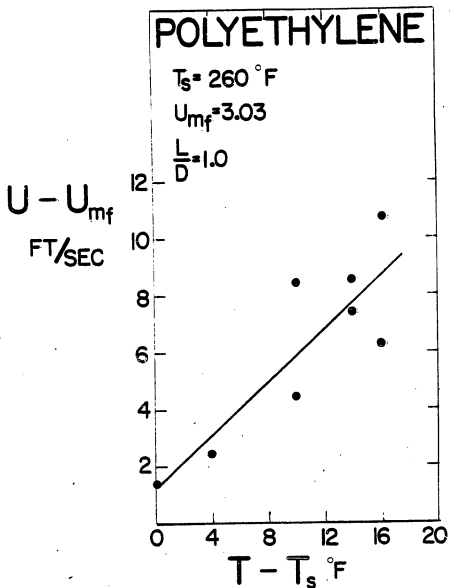


F. VIII

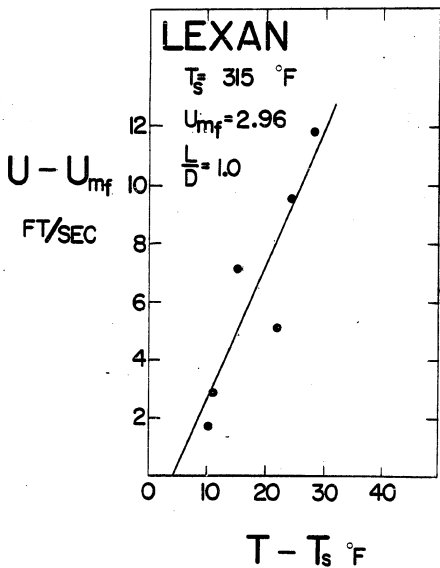




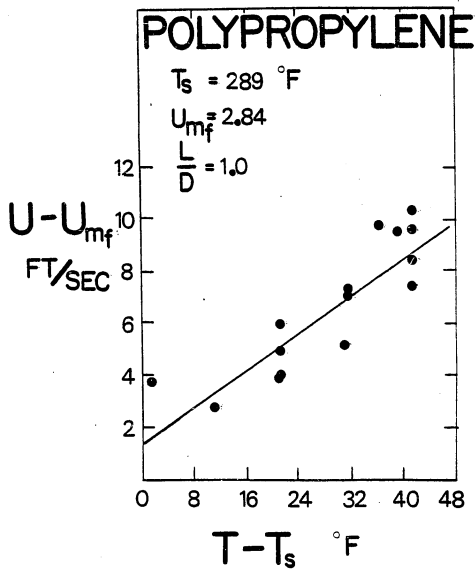
F.X



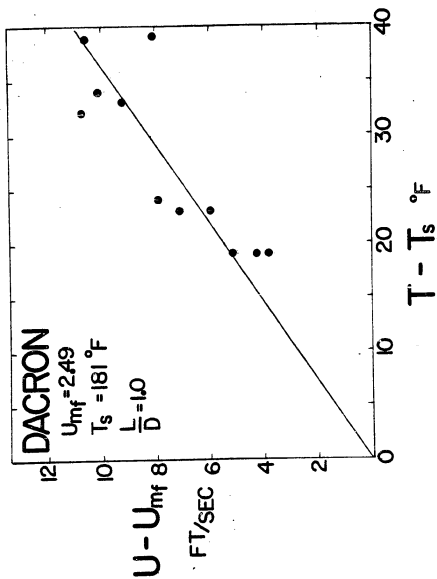
F. XI



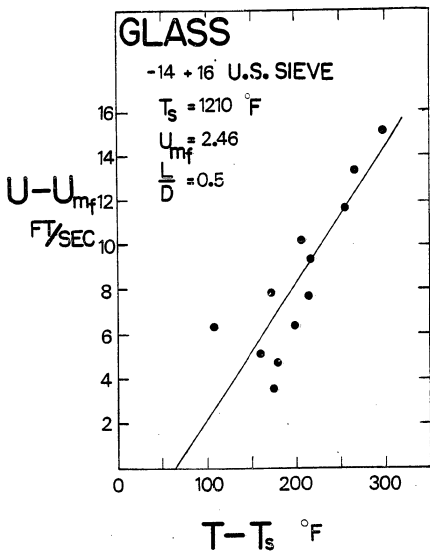
F.XII



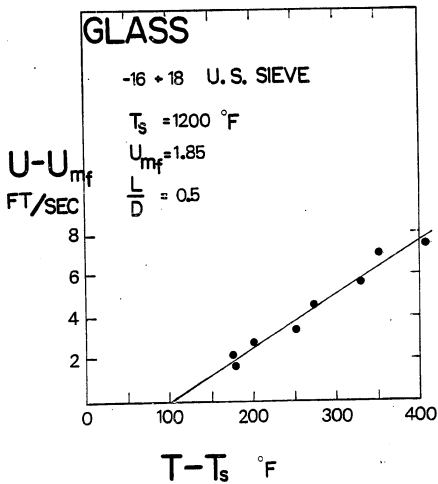
F. XIII



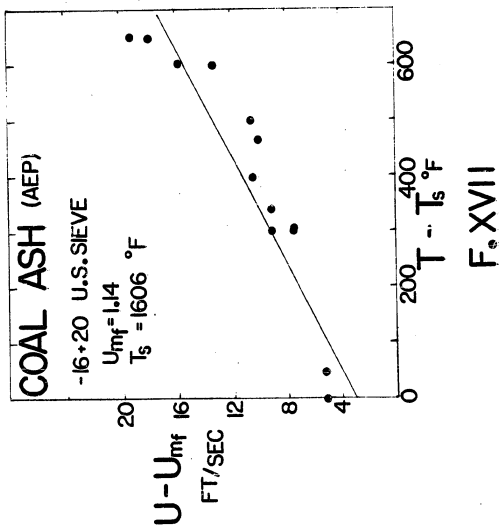
F. XIV

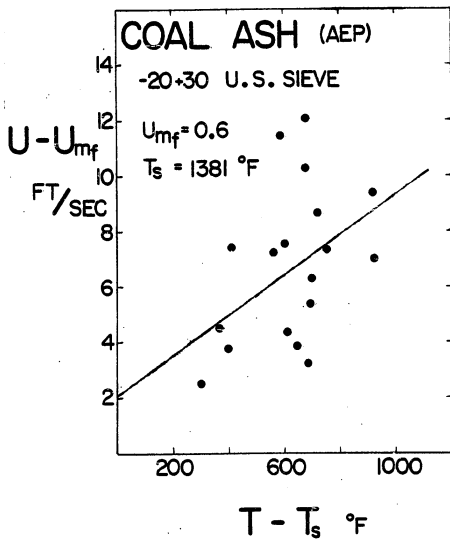


F.XV

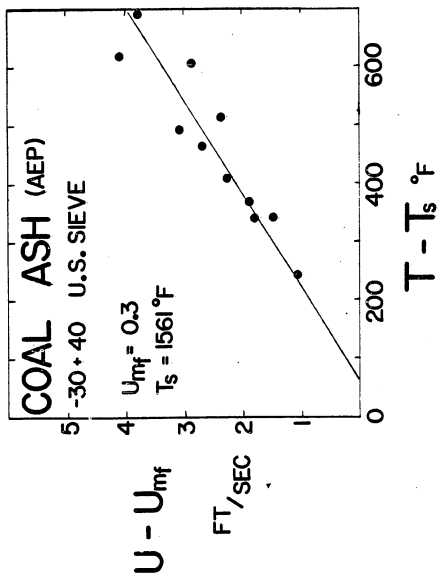


F. XVI

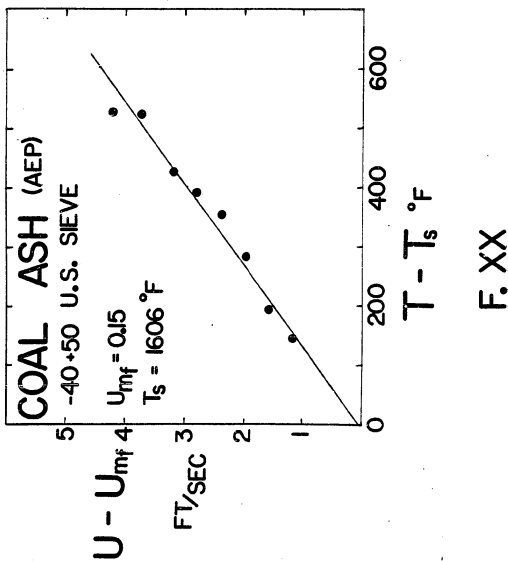


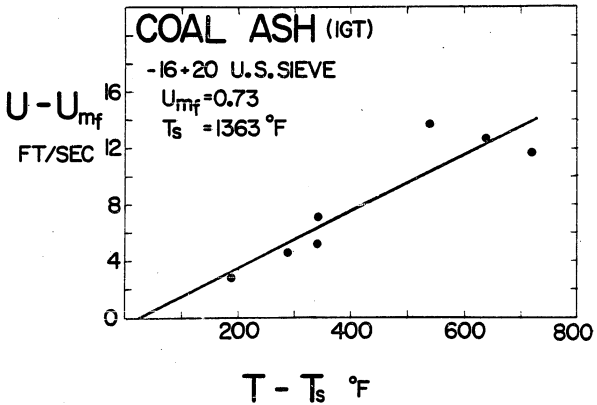


F. XVIII

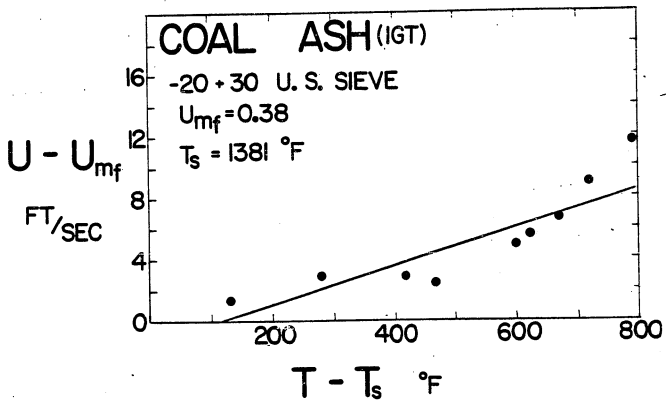


F. XIX

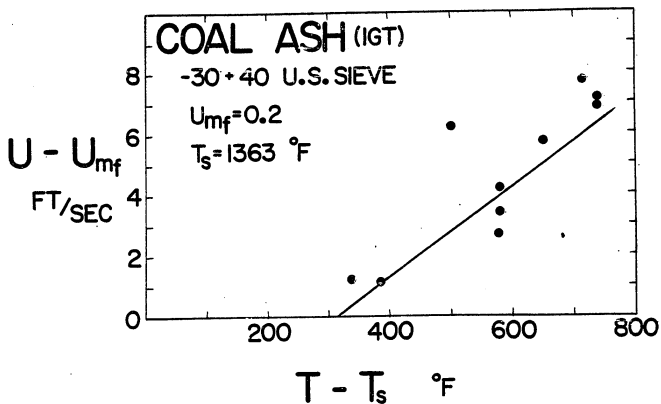




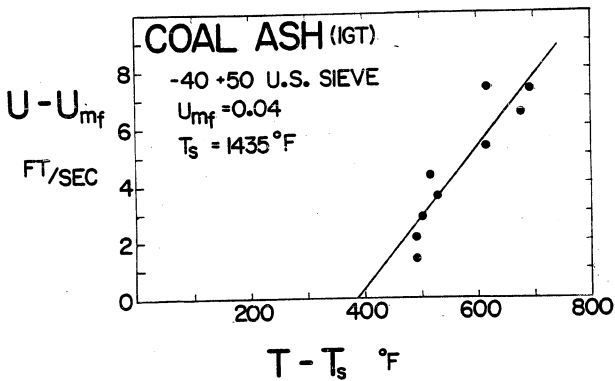
F. XXI



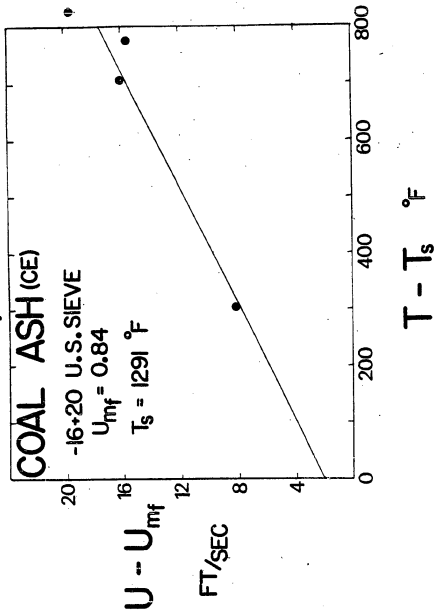
F. XXII



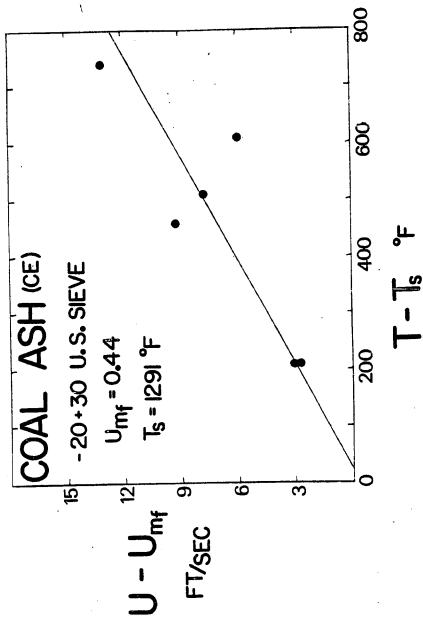
F. XXIII

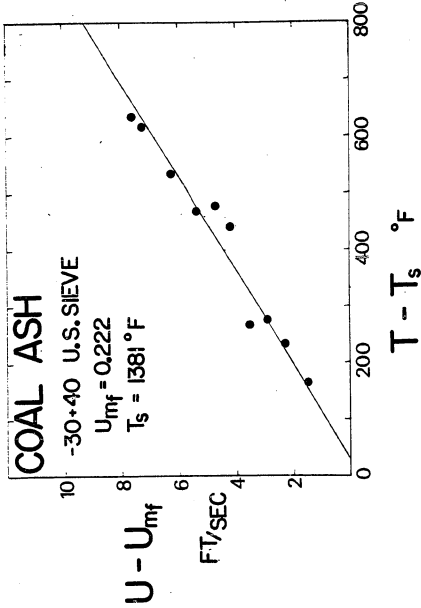


F. XXIV

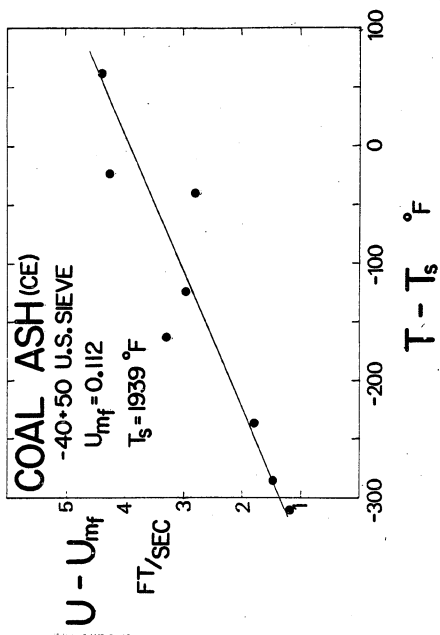


F. XXV

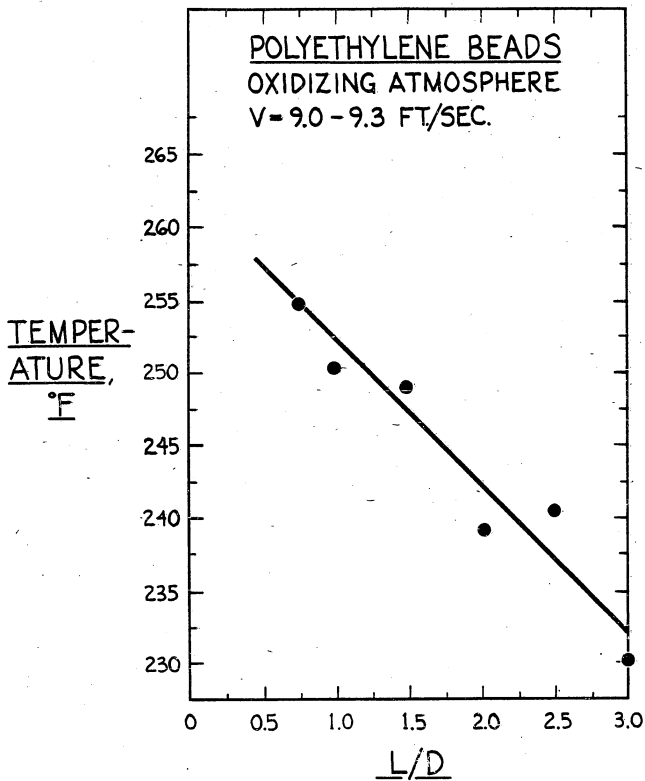
**F. XXVI**



F. XXVII

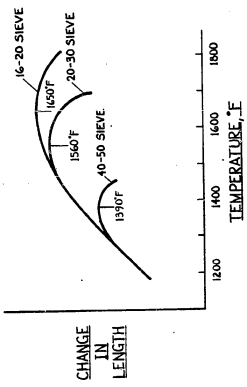


F. XXVIII



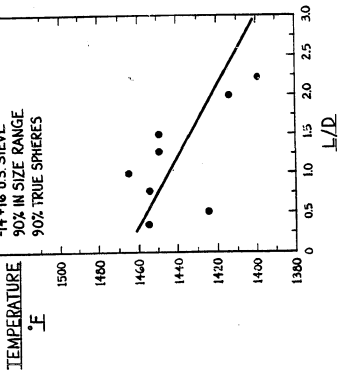
F. XXIX

SINTERING STUDIES — COPPER SHOT
OXIDIZING ATMOSPHERE

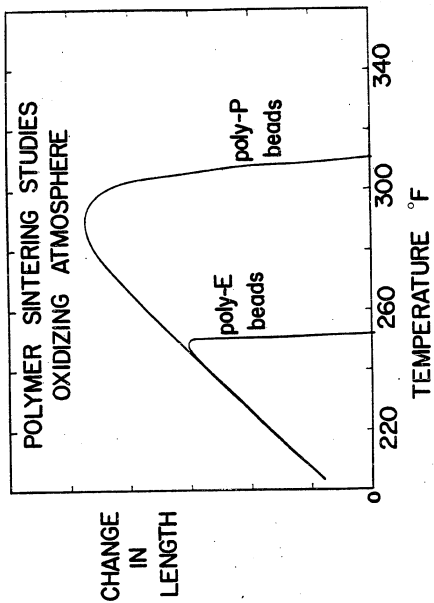


F. XXXI

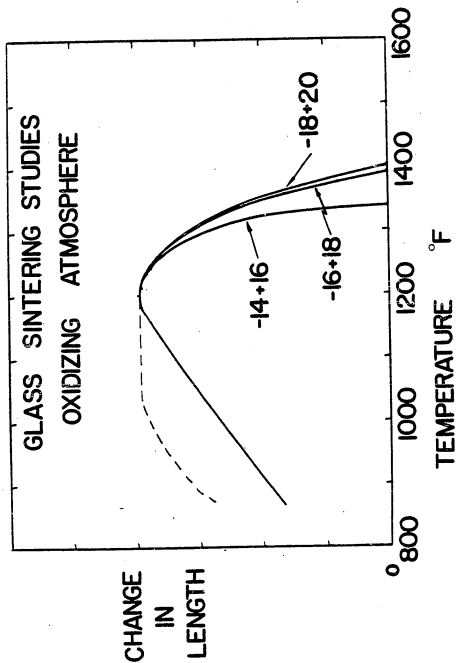
GLASS SPHERES
OXIDIZING ATMOSPHERE
-14 + 16 U.S. SIEVE
90% IN SIZE RANGE
90% TRUE SPHERES



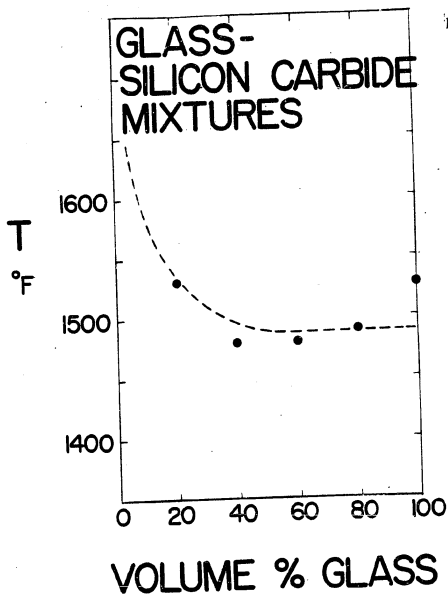
F. XXX



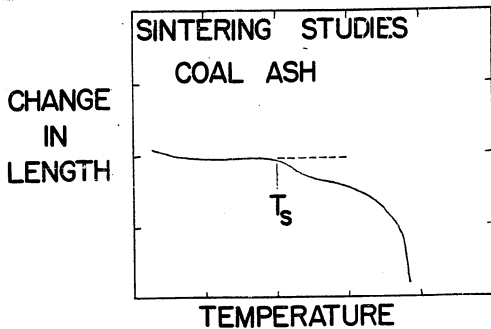
F. XXXII



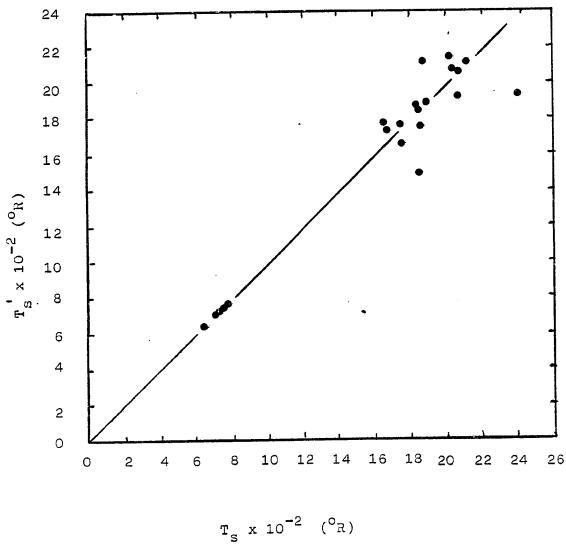
F. X X X III



F. XXXIV



F. XXXV



F. XXXVI

APPENDIX II

DEFLUIDIZATION DATA

Copper Particles

Size: - 16+20 U.S. sieve

 $L/D = 0.5$ $T_s = 2110^{\circ}\text{R}$ $U_{mf} = 3.93 \text{ ft/sec}$

<u>Temperature</u>	<u>Velocity</u>
1800 ^o F	8.1ft/sec
1800	8.1
1760	6.7
1725	5.3
1625	4.5
1805	7.5
1720	4.6
1655	4.0
1845	8.9
1880	9.7
1775	7.4
1800	7.2
1810	7.2
1885	10.96

Copper Particles

Size: - 20+30 U.S. Seive

L/D = 0.5

$T_s = 2010^{\circ}\text{R}$

Umf = 2.20 ft/sec

Temperature

1785^oF

1755

1720

1790

1700

1780

Velocity

7.03 ft/sec

4.89

3.84

8.93

2.95

9.57

Copper Particles

Sieve: - 40+50 U.S. Sieve

$L/D = 0.5$

$T_s = 1841^{\circ}R$

$U_{mf} = 0.61 \text{ ft/sec}$

<u>Temperature</u>	<u>Velocity</u>
1670 ^o F	4.63
1685	5.6
1755	6.98
1700	2.96
1650	5.19
1610	2.83
1740	7.95
1800	9.84
1435	3.66
1820	6.1

Polyethylene Beads

$$d_p = 0.244 \text{ cm}$$

$$L/D = 1.0$$

$$T_s = 704^\circ\text{R}$$

$$U_{mf} = 2.21 \text{ ft/sec}$$

Temperature245^oF

275

250

260

240

250

255

255

258

250

Velocity

11.56 ft/sec

11.63

7.23

15.79

5.34

9.26

11.31

12.41

14.65

5.37

Bed Depth EffectL/D

1

2

3

1.5

2.5

0.75

Temperature250^oF

238

230

248

240

255

Velocity

9.26 ft/sec

9.02

9.13

9.17

9.32

9.29

POLYETHYLENE BALLS

$$d_p = 0.317 \text{ cm}$$

$$L/D = 1.0$$

$$T_s = 720 \text{ }^\circ\text{R}$$

$$U_{mf} = 3.03 \text{ ft/sec}$$

TemperatureVelocity

270 $^\circ\text{F}$	11.56 ft/sec
270	7.46
264	5.43
260	4.47
276	13.8
275	11.64
275	10.52
276	9.38

Polypropylene Beads

$$d_p = 0.302 \text{ cm}$$

$$L/D = 1.0$$

$$T_s = 749^\circ\text{R}$$

$$U_{mf} = 2.84 \text{ ft/sec}$$

TemperatureVelocity

350°F	12.54 Ft/sec
285	8.59
310	7.8
290	6.64
310	6.82
300	5.54
320	7.94
320	10.12
330	11.3
325	12.6
310	6.83
320	6.92
310	7.85
328	12.46
330	13.23
320	10.09
330	10.22
310	8.88

DACRON
(Polyethylene Terephthalate)

$$d_p = 0.1984 \text{ cm}$$

$$L/D = 1.0$$

$$T_s = 641^\circ \text{R}$$

$$U_{mf} = 2.49 \text{ ft/sec}$$

<u>Temperature</u>	<u>Velocity</u>
220 ^{°F}	10.56 ft/sec
215	12.59
204	8.48
200	6.68
205	10.41
200	6.29
220	13.08
213	13.12
214	11.69
200	7.64
204	9.55

LEXAN

$$d_p = 0.256 \text{ cm}$$

$$L/D = 1.0$$

$$T_s = 775^\circ\text{R}$$

$$U_{mf} = 2.96 \text{ ft/sec}$$

Temperature339^oF

337

343

330

326

325

Velocity

12.59 ft/sec

8.13

14.98

10.21

5.93

4.9

GLASS

Size: -14+16 U.S. sieve

L/D = 0.5

 $T_s = 1670^{\circ}\text{R}$

Umf = 2.46 ft/sec

<u>Temperature</u>	<u>Velocity</u>
1370 ^o F	7.48 ft/sec
1320	8.86
1420	12.51
1470	14.18
1475	15.9
1390	7.12
1385	5.96
1380	10.41
1425	11.91
1500	17.62
1405	8.84
1425	10.23

BED DEPTH EFFECT

<u>L/D</u>	<u>Temperature</u>	<u>Velocity</u>
0.5	1425 ^o F	11.91 ft/sec
1	1465	11.86
1.5	1450	11.95
2	1415	11.76
0.75	1455	12.02
0.35	1455	11.99
2.25	1400	11.64
1.3	1450	11.92

GLASS

Size: -16+18 U.S. sieve

L/D = 0.5

 $T_s = 1660^{\circ}\text{R}$

Umf = 1.85 ft/sec

Temperature1450^oF

1530

1550

1400

1375

1380

1610

1470

Velocity

5.32 ft/sec

7.43

8.9

4.56

3.95

3.45

9.28

6.41

BED DEPTH EFFECTL/D

0.5

1.0

1.5

2

1

0.75

0.3

Temperature1550^oF

1410

1430

1380

1400

1430

1430

Velocity

8.9 ft/sec

8.07

8.97

8.78

8.61

8.68

8.73

COAL ASH (AEP)

Size: -16+20 U.S. sieve

L/D = 0.178

 $T_s = 2066^{\circ}\text{R}$

Umf = 1.14 ft/sec

<u>Temperature</u>	<u>Velocity</u>
2100 ^o F	11.8 ft/sec
1900	8.8
1650	6.36
1945	10.46
1600	6.34
2200	14.56
2000	11.59
1910	8.59
2065	11.44
2200	16.99
1900	10.26
2250	19.15
2260	20.7
2250	19.64

COAL ASH (AEP)

Size: - 20+30 U.S. Sieve

L/D = 0.178

 $T_s = 1841^{\circ}\text{R}$

Umf = 0.6 ft/sec

TemperatureVelocity

1795 ^{°F}	8 ft/sec
1750	5.1
1970	12.1
1690	3.05
1980	8.22
1780	4.4
2300	7.5
2100	9.28
2025	4.5
2070	3.82
1990	4.88
2070	5.96
2075	6.89
2125	7.96
1750	7.86
2050	10.91
2050	12.73
2300	10.0

COAL ASH (AEP)

Size: -30+40 U.S. Sieve

 $L/D = 0.178$ $T_s = 2021^{\circ}\text{R}$ $U_{mf} = 0.3 \text{ ft/sec}$ TemperatureVelocity

2050 ^o F	3.41 ft/sec
2175	3.18
1900	2.14
1800	1.36
2075	2.68
1900	1.78
1930	2.16
1970	2.57
2025	3.00
2250	4.09
2180	4.38

COAL ASH (AEP)

Size: -40+50 U.S. Sieve

L/D = 0.178

 $T_s = 2066^{\circ}\text{R}$

Umf = 0.152 ft/sec

TemperatureVelocity

1950 ^o F	2.55 ft/sec
1890	2.13
1800	1.71
2000	2.97
2030	3.38
2130	3.91
1750	1.33
2135	4.31

COAL ASH (IGT)

Size: -16+20 U.S. sieve

$L/D = 0.178$

$T_s = 1823 \text{ } ^\circ\text{R}$

$U_{mf} = 0.725 \text{ Ft/sec}$

Temperature

2080^oF
1700
1700
2000
1650
1900
1550

Velocity

12.42 ft/sec
5.86
7.83
13.37
5.35
14.54
3.6

COAL ASH (IGT)

Size: - 20 +30 U.S sieve

 $L/D = 0.178$ $T_s = 1841^{\circ}R$ $U_{mf} = 0.38 \text{ ft/sec}$ Temperature2100^oF
1800^oF
2050^oF
1660^oF
1510^oF
1850^oF
2000^oF
2170^oF
1980^oFVelocity9.28 ft/sec
3.27
6.97
3.84
1.78
2.79
5.94
11.9
5.16

Coal ASH (IGT)

Size: - 30 + 40 U.S. sieve

$L/D = 0.178$

$T_s = 1823 \text{ }^\circ\text{R}$

$U_{mf} = 0.2 \text{ ft/sec}$

TemperatureVelocity

2100 ^o F	7.11 ft/sec
1750	1.33
1975	5.14
2140	7.3
1700	1.63
2015	5.98
1940	4.35
1945	3.63
1940	2.9
2100	2.11

COAL ASH (IGT)

Size: - 40+50 U.S. sieve

$L/D = 0.178$

$T_g = 1895 \text{ }^\circ\text{R}$

$U_{mf} = 0.041 \text{ ft/sec}$

Temperature

2125^oF

2110

2050

1950

1965

1935

1925

1925

2050

Velocity

7.34 ft/sec

6.44

5.3

4.37

3.66

2.89

2.16

1.44

7.28

COAL ASH (CE)

Size: -16+20 U.S. Sieve

$L/D = 0.178$

$T_s = 1751 \text{ } ^\circ\text{R}$

$U_{mf} = 0.842 \text{ ft/sec}$

<u>Temperature</u>	<u>Velocity</u>
2070 ^o F	16.5 ft/sec
1600	8.96
2125	20.14
2000	16.93

COAL ASH (CE)

Size: -20 + 30 U.S. Sieve

L/D = 0.178

$T_s = 1751 \text{ }^\circ\text{R}$

$U_{mf} = 0.438 \text{ ft/sec}$

<u>Temperature</u>	<u>Velocity</u>
2030 ^o F	13.53 ft/sec
1750	9.61
1800	8.19
1900	6.41
1500	3.55
1500	3.2

COAL ASH (CE)

Size: -30 + 40 U.S. Sieve

$L/D = 0.178$

$T_s = 1841 \text{ } ^\circ\text{R}$

$U_{mf} = 0.222 \text{ ft/sec}$

<u>Temperature</u>	<u>Velocity</u>
2000 ^o F	7.43 ft/sec
1920	6.47
1850	5.58
1860	4.9
1650	3.82
1660	3.2
1615	2.51
1550	1.82
2020	7.86
1825	4.41

COAL ASH (CE)

Size: -40 + 50 U.S. Sieve

$L/D = 0.178$

$T_s = 2399^{\circ}\text{R}$

$U_{mf} = 0.112 \text{ ft/sec}$

<u>Temperature</u>	<u>Velocity</u>
1780 ^o F	3.38 ft/sec
1920	4.3
1900	2.85
2000	4.46
1820	3.1
1700	1.95
1630	1.26
1650	1.59

GLASS - SILICON CARBIDEMIXTURES

Glass: -16 + 18 U.S. Sieve

Silicone Carbide : -14 + 24 U.S. Sieve

L/D 0.5

<u>Volume % Glass</u>	<u>Temperature</u>	<u>Velocity</u>
100	1530 °F	7.43 ft/sec
80	1490	7.43
60	1480	7.12
40	1480	7.24
20	1530	7.37

APPENDIX IIICOAL ASH COMPOSITIONS

	<u>AEP</u>	<u>IGT</u>	<u>C E</u>
Silica %	42.5	44.06	26.9
Iron Oxide %	24.9	37.75	7.75
Aluminum Oxide %	25.7	13.84	16.14
Calcium Oxide%	2.8	1.84	16.8
Magnesium Oxide %	3.0	1.05	3.2
Sulfur Tri-Oxide %	-	-	19.11

APPENDIX IV : COEFFICIENTS FOR DEFLUIDIZATION CURVES

$$(U-U_{mf}) = A(T-T_s) + B$$

A(FT/SEC⁰F)
B(FT/SEC)

<u>SYSTEM</u>	<u>A</u>	<u>B</u>	<u>regression coefficient</u>
Copper -16+20 U.S. Sieve	0.03	0.0	0.95
Copper -20+30 U.S. Sieve	0.07	-9.65	0.91
Copper -40+50 U.S. Sieve	0.0134	0.8681	0.6593
Polyethylene Beads	0.8786	-0.1363	0.9505
Polyethylene Spheres	0.4612	1.295	0.854
Polypropylene Beads	0.176	1.472	0.8242
Dacron	0.27	0.052	0.86
Lexan	0.467	-2.06	0.886
Glass -14+16 U.S. Sieve	0.06	-3.87	0.84
Glass -16+18 U.S. Sieve	0.03	-2.53	0.98
Coal Ash(AEP) -16+20 U.S. Sieve	0.021	2.96	0.92
Coal Ash(AEP) -20+30 U.S. Sieve	0.007	2.47	0.41
Coal Ash(AEP) -30+40 U.S. Sieve	0.006	-0.362	0.93
Coal Ash(AEP) -40+50 U.S. Sieve	0.0073	0.065	0.99
Coal Ash(IGT) -16+20 U.S. Sieve	0.0202	-0.50	0.91
Coal Ash(IGT) -20+30 U.S. Sieve	0.0132	-1.58	0.87
Coal Ash(IGT) -30+40 U.S. Sieve	0.015	-4.69	0.95
Coal Ash (IGT) -40+50 U.S. Sieve	0.025	-9.65	0.92
Coal Ash (CE) -16+20 U.S. Sieve	0.0194	2.0503	0.97
Coal Ash (CE) -20+30 U.S. Sieve	0.0159	-0.2475	0.87
Coal Ash (CE) -30+40 U.S. Sieve	0.012	-0.3855	0.98
Coal Ash (CE) -40+50 U.S. Sieve	0.0082	3.8908	0.93

APPENDIX V. AGGLOMERATE EXAMINATION

The agglomerates that were formed, when the bed defluidized, were later removed and examined in the hope that they would suggest the mechanisms by which the defluidization took place. Several types of photographs were made, in addition to the physical examination of the particles. Some of these photographs were made using a standard single lens reflex camera with, either a fifty millimeter macro lens, or a microscope attachment. Other photographs were made using a scanning electron microscope (SEM). All of the micrographs and SEM pictures presented in this section were furnished by the E. I. duPont de Nemours Co., Inc., Wilmington, Delaware.

Utmost care was necessary in removing the agglomerates from the reactors. It was found that many of the agglomerates would fall apart under the smallest pressure. This suggested that the bonds, between the individual particles were very weak, and that true bonding between particles never took place. This fact also suggests possible industrial application where material could be removed from a fluidized bed by agglomeration and then easily broken apart in another bed to be refluidized.

In most cases, the agglomerates examined contained particles that closely resembled the individual feed particles. Depending upon the mechanism by which the bond zone between the particles was formed, there would either be substantial deformation or none. Crystalline, or metallic materials were found to form bond zones by diffusion of material to the zone. This diffusion did not alter the shape of the original individual particle. For example, the copper agglomerates were made from in-

dividual particles that had not appeared to change shape from before defluidization. Glass and polymeric materials formed bond zones by a viscous flow mechanism which tended to alter the original particle shape significantly. The mechanism by which the coal ash particles agglomerated seemed to depend on the defluidization temperature they were subjected to. At lower temperatures, near the "initial sticky temperature", the ash particles tend to form bonds by diffusion. At higher temperature however, viscous flow was evident at temperatures inbetween a combination of these mechanisms cause the particles to bond.

Superficial examination of these agglomerates indicates that the defluidization phenomenon, caused by the formation of bonds, to be a surface phenomenon. In cases where substantial particle deformation and material movement toward the bond zone occurred, it is believed that most, if not all of the deformation occurred after defluidization as the bed slowly cooled.

The following are descriptions of the agglomerate pictures found at the end of this section. Numbers correspond to those found below each picture:

1. Copper agglomerate showing several hundred individual particles (-16+20 U. S. sieve size) bonded together. These particles were easily broken apart by hand. Due to operation in an oxidizing atmosphere, the copper particles had an oxide coating. The individual particles have clearly retained their original shape since the mechanism for sintering, in this case, was diffusion.

2. Several copper agglomerates made from particles, as above, are shown. Again note the lack of particle deformation. Agglomerates were found in many shapes and sizes but no information could be obtained from these findings due to the fact that, after the bed defluidized, the fluidizing gas (air) continued to pass through it and this caused the bed to break into smaller agglomerates as it was cooled. Most of the beds that were removed "whole" showed signs of "rat holes" or channels being blown through them.

3. This is a cross sectional view, magnification 100x, showing the bonding zone of three copper particles. The dark ring, surrounding the particles, is an oxide layer caused by operation in an oxidizing atmosphere. The oxide coating, bonding the particles, seems rather porous which could also account for the weakness of the bonding.

4. Similar to above, magnification 200x, showing bonding zone of two particles. Note that no particle deformation appears to have occurred in the region of bonding. This is typical when sintering occurs in metals by diffusional mechanisms. In addition, there seems to be no effect of this bonding on the

majority of the particle other than the bonding zone. This sintering appears to be solely a surface phenomenon.

5,6. These cross sections, magnification 125x and 400x, show the bond zone more clearly. The point of bonding appears sharp and no material has moved into voids created. An acute angle is formed between the two particles. This acute angle is only formed when there is sintering by a diffusional mechanism. If the sintering had occurred by viscous flow, the points of contact would be rounded and smooth. Note that no densification has begun even in the bond zone area, where a very high porosity is apparent.

7. Agglomerates made from -16+20 U. S. sieve glass spheres. Concave section in upper left is part of what was a "blow hole". The glass agglomerates were found to be much more strongly bonded than were the copper agglomerates but could still be broken apart easily by hand. Particles that were broken off were found to have undergone substantial deformation in the bond zone areas.

8,9,10. Closer examination of the glass agglomerates shows that the glass appears to have "flowed" to the bond zones. In some cases, massive deformation of the

entire particle is observed. This behavior is evidence of sintering by viscous flow.

11,12. Scanning electron micrographs, magnification 30x and 50x, show the bond zone between two glass particles. Note that the bond zones formed are created by what appears to be a flow of material between the particles and not by actual contact. The points of contact at the bonding zone are smooth and no acute angle is formed as was the case with the copper particles. Although these micrographs show substantial particle deformation, it is believed most of the deformation took place after defluidization as the bed was allowed to cool slowly.

13,14. Scanning electron micrographs, magnification 30x and 50x, show the bond zone between two polyethylene spheres. Note the bond zone formed is similar to the bond zones formed between the glass particles. Material from each of the spheres has extended from the sphere toward the other forming bond. The bond zone seems to be made up of many fiber type strands. This may be due to the polymeric nature of the material. Linear polyethylene has a chain type structure and these fibers may be due to chains joining from one particle to another.

- 15,16. Scanning electron micrographs, magnification 10x, showing bonding zone between two polyethylene beads. These polyethylene beads were found not to deform significantly due to defluidization, except for the rounding of sharp corners. The second micrograph shows the bonding region as two particles are broken apart. Note the fibers left hanging after the bond was broken. Bonds between polyethylene particles were quite strong and could not easily be broken by hand.
- 17,18. Agglomerates of extruded polypropylene pellets are shown. These agglomerates were fairly easily broken apart by hand with moderate pressure. No deformation of the particles was found even though they originally had sharp corners. Visual observation showed no deformation even at these corners. Large agglomerates removed from the bed, after defluidization, were found to be quite porous and contain many "blow holes".
- 19,20,21,22. Coal ash agglomerates (-16+20 U. S. sieve, American Electric Power dry bottom boiler). These ash agglomerates are extremely easily broken apart, even though in some regions the ash seems to have been in a molten state. The presence of evidence of a molten state could have been caused by localized hot spots after defluidization.

It is believed that the ash became molten only after defluidization. This is supported by the fact that most of the agglomerate showed no sign of having passed through a molten state, and the almost uniform temperature throughout the fluidized bed just before defluidization.

In the upper right part of picture 19 and lower right part of picture 20, "blow holes" were formed through the agglomerate. In picture 20, individual particles were broken off just by placing the agglomerate down to take this picture.

Picture 21 shows several small agglomerates along with the individual particles that have broken from them. Picture 22 shows three larger agglomerates.

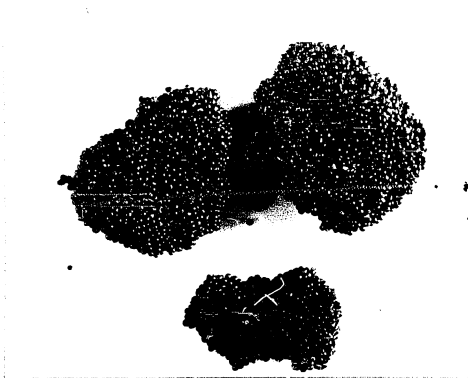
In many cases the entire bed would contain just one very large ash agglomerate which could not be removed in total, due to the weak bonds between the individual ash particles.

23,24. Coal ash agglomerates (-16+20 U. S. sieve, American Electric Power dry bottom boiler). These are microscopic photographs of agglomerates from picture 21. It is interesting to note that the individual particles of ash appeared to be agglomerates of much finer size when examined microscopically before defluidization experiments were made. The bond zones between these "ultra-fines" that made up each of the in-

dividual feed particles were easily seen. However, after defluidization when the agglomerates were examined, it was not apparent that the original individual particles were themselves agglomerates. The bond zones had been smoothed due to material flow to it. It appeared as if the individual particle had undergone densification due to the high temperatures experienced during the defluidization experiments. If this is so, then in fact, two sintering operations were taking place at the same time: the weak bonding of the individual feed particles to each other causing large agglomerates and eventually defluidization and the densification of these same individual feed particles into a solid mass.



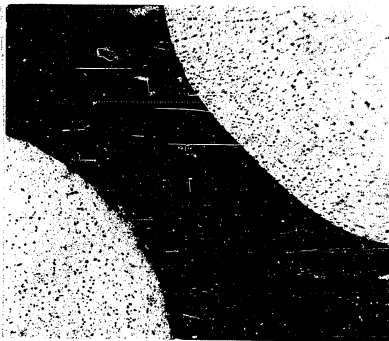
1



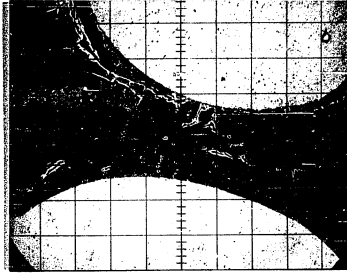
2



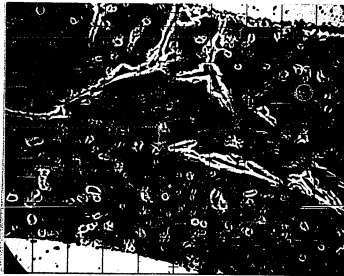
3



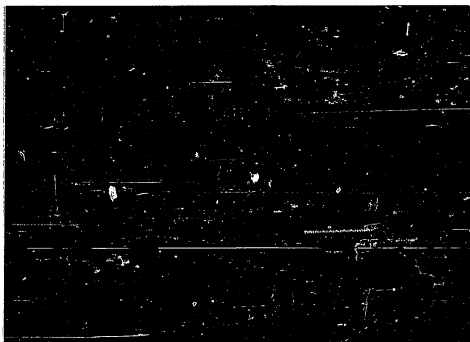
4



5



6



7



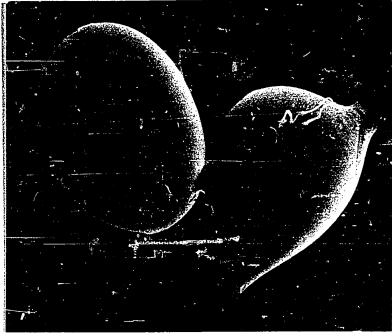
8



9



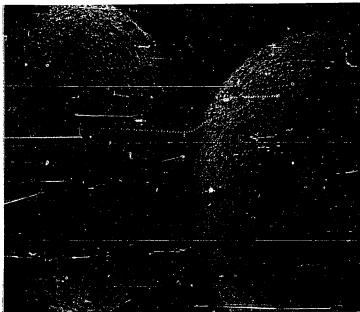
10



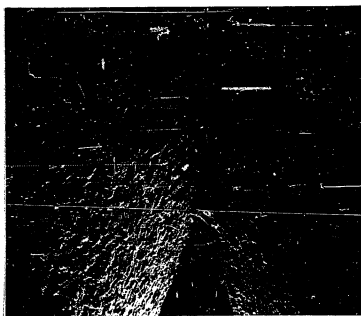
11



12



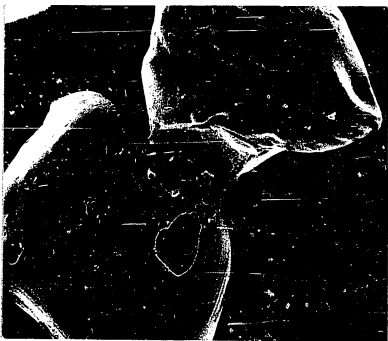
13



14



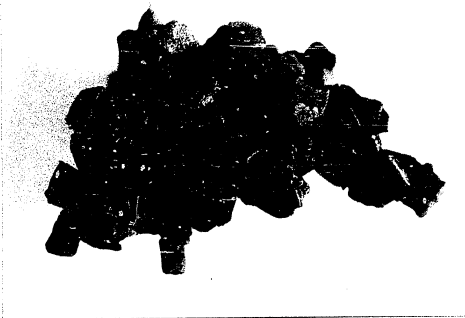
15



16



17



18



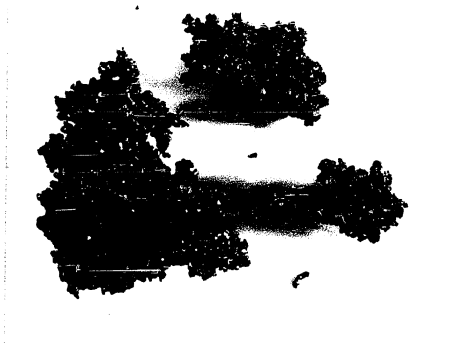
19



20



21



22



23



24

APPENDIX VI. HIGH SPEED PHOTOGRAPHY

High speed photography was used to capture the motion of the particles as the fluidized bed approached the high temperature defluidization limit. It was hoped that, by studying the motion of the individual particles, greater understanding of the mechanism of defluidization would be achieved. Time expansions of almost fifty times were achieved at the highest speeds. However, due to lighting requirements and aperture openings, the depth of field was severely limited.

The two inch directly heated fluidized bed was used for this photography work since the pictures could be taken through the transparent quartz tube. The solid used was a fine copper powder (-40+50 U. S. sieve) which exhibited aggregative fluidization. The photography window was approximately one-half inch square, with a depth of field slightly less than one-half inch. It was required to take an abundant amount of film in order to obtain a single good print, showing particle motion. The results justify the time and effort spent in this endeavor. The problem here was that, once the camera was switched on, it could not be stopped until all the film was exposed. If this was not timed exactly to the point of defluidization, all that would be obtained would be shots of single particle movement without any agglomeration, or a bed that had already defluidized.

At the beginning of the film that was produced the bed was still well below the high temperature limit for defluidization and contained only single particles. Vigorous activity is apparent as particles pass so quickly that they become a blur, even at the high camera speed used. As was mentioned before, due to the small depth of

field, only particles in the very near section of bed were clearly visible.

As the high temperature limit was approached, two and three particle agglomerates began to appear throughout the bed. It is interesting to discuss the behavior of these agglomerates when they collide with one another. At this temperature the bed will not defluidize so that larger agglomerates will not be formed (the larger agglomerates possibly causing defluidization). When the agglomerates collided, it was found that they tend to break apart into smaller pieces. Hence, there seems to be two processes occurring of opposite effect just below the defluidization temperature: the adhesion of two single particles to each other, or a two particle agglomerate to a third particle and the breakup of the two and three particle agglomerates as they collide in the bed. It is evident that, if the fluidization velocities were raised, the rate of agglomerate breakup would be substantially greater than that of formation and a higher temperature would be necessary to maintain the same relative number of agglomerates.

As the temperature increased, the average size of agglomerates in the bed was found to increase as the rate of agglomerate formation began to greatly increase relative to their breakup. This is believed due to an increased rate of particle sintering at the higher temperature. However, since the bed was very close to the point of defluidization, the increase in agglomerate average size could have been an indication of "incipient defluidization", rather than just increasing temperature.

Just before the bed defluidized, the activity of the particles began to decrease. The entire bed seemed as if it now had to overcome some heavy weight that was

placed upon it and began to slug violently. The agglomerates started to grow to enormous sizes, containing what appeared to be several hundred particles. When two of these large agglomerates collided, many smaller agglomerates were created by material being broken off the parent agglomerate. The majority of the particles of each agglomerate remained intact to form a new agglomerate much larger than either of the two original ones. As these agglomerates grew and grew, the behavior of the bed did not resemble anything like normal

fluidization. It was more like a tube containing several spheres of about half the tube diameter fluidized just above the minimum velocity.

The entire bed would then just collapse into a solid mass for a split second. At that point, the fluidizing gas would crack through the bed, causing some movement and fluidization of small two and three particle agglomerates around "blow holes" and "channels" that were created. These small agglomerates would almost immediately adhere to the defluidized bed mass.

It should be remembered that the entire process described here occurred over only a few seconds of time, and was observed only with the use of high speed photography. The temperature differences below the high temperature limit, where agglomeration first begins, were only a few degrees. There was no evidence of any agglomeration much below this temperature. Film shot just before the point of defluidization, which was of no use in this analysis, showed the bed did not contain any agglomerates, and single particles coming in contact with one another did not adhere.

It was impossible to obtain any quantitative data from this high speed photographic analysis for two reasons. The first was that only a small region of the

bed could be seen and only the section near the tube wall. This was due to the very limited depth of field. Particles toward the center and rear of the bed were not in focus. In addition, the true speed of the camera was not known. Due to the short length of each film, and the high speed used, it was not until almost the end of the film length that the actual set film speed was reached. Although no quantitative data could be obtained, a good qualitative picture of how particles behave in an agglomerating bed was established.

REFERENCES

- P. Angevine, Dorr-Oliver, Stamford, Connecticut, personal communication with A. M. Squires (1971).
- D. H. Barnhart, P. C. Williams, Babcock and Wilcox, Alliance, Ohio, "The Sintering Test, An Index to Ash-Fouling Tendency", Transactions of the ASME (August 1956).
- R. F. Blanks, H. L. Kennedy, The Technology of Cement and Concrete: Volume I: Concrete Materials, John Wiley and Sons, New York (1955).
- N. T. Cankurt, "Fluidization of Sticky Particles - Studies Toward Improved Techniques for Gasifying Coal", Industrial Briefing, CUNY, January 16-17, 1974.
- N. T. Cankurt, "Fluidization of Sticky Particles - Studies Toward Improved Techniques for Gasifying Coal", Second Annual Industrial Briefing, Americana Hotel, New York City, January 13-14, 1975.
- P. Cosar, "The Combustion of Carbon in a Fluidized Bed", Arts et Manufacturers, No. 196 (April 1969).
- R. H. Demmy, UGI Industries, Kingston, Pennsylvania, "Ignifluid Boiler for an Electric Utility", talk at the A.I.Ch.E. Meeting, Cincinnati, Ohio (May 1971).
- F. J. Dent, personal communication with A. M. Squires (1958).
- F. J. Dent, "Discussion" of Squires (1961), Trans. Inst. Chem. Engrs. (London), Vol. 39, pp. 22-23 (1961).
- S. Ehrlich, J. W. Bishop, J. S. Gordon, E. B. Robinson, A. Hoerl, Pope, Evans and Robbins, "Particulate Emissions from a High Temperature Fluidized Bed Fly Carbon Burner", A.I.Ch.E., New York (November 1972).

- A. A. Godel, "Process for the Gasification of Granulated Fluidized Bed of Carbonaceous Material, Over Moving, Sloping, Horizontal, Continuous Grate", U. S. Patent No. 2,866,696 (December 30, 1958).
- A. A. Godel, "Ten Years of Experience in the Technique of Burning Coal in Fluidized Bed", *Revue General de Thermique*, Vol. 5, 349-359 (1966).
- A. A. Godel, Societe Anonome Activit, Paris, France, personal communication with A. M. Squires (1968).
- W. M. Goldberger, Batelle Memorial Institute, Columbus, Ohio, "Collection of Fly Ash in a Self-Agglomerating Fluidized Bed Coal Burner", paper presented at ASME, Pittsburgh, Pennsylvania (November 1967).
- R. D. Harvey, S. M. Masters, Illinois State Geological Survey, Urbana, Illinois, "Ash Agglomerates from Ignifluid Gasifiers of Coal", (February 1974).
- R. W. Hiteshue, S. Friedman, R. Madden, "Hydrogasification of High-Volatile A Bituminous Coal", U. S. Bureau of Mines Rept. Invest. No. 6376 (1964).
- L. Jequier, L. Longchambon, G. Van de Putte, "The Gasification of Coal Fines", J. Inst. Fuel, Vol. 33, 584-591 (1960).
- W. Kramer, Fuller Company, Catasqua, Pennsylvania, personal communication with A. M. Squires (1961).
- B. G. Langston, F. M. Stephens, Jr., "Self Agglomerating Fluidized Bed Reduction", J. of Metals, Vol. 12, 312-316 (1960).
- R. Pyzel, "Cement Manufacture", U. S. Patent 2,776,132 (January 1, 1957).
- R. Pyzel, "Hydraulic Cement Process", U. S. Patent 2,874,950 (February 24, 1959).

- R. Pyzel, "Apparatus for Cement Manufacture", U.S. Patent 2,977,105 (March 28, 1961a).
- R. Pyzel, "Particle Size Control", U. S. Patent 2,981,531 (April 25, 1961b).
- A. M. Sadler, "High Temperature Fluidized Bed Process for the Production of Portland Cement", paper presented at A.I.Ch.E. Meeting, New York (November 1967).
- A. M. Squires, "Agglomerating Coal Hydrocarbonization Process", U. S. Patent 3,347,561 (April 8, 1969a).
- A. M. Squires, "Process for Pyrolyzing a Solid or Liquid Hydrocarbonaceous Fuel in Fluidized Bed", U. S. Patent 3,579,327 (August 3, 1971).
- A. M. Squires, "Process and Apparatus for Desulfurizing Fuels", U. S. Patent 3,481,384 December 2, 1969b).
- A. M. Squires, R. A. Graff, M. Pell, "Desulfurization of Fuels with Calcined Dolomite: I. Introduction and First Kinetic Results", paper presented at A.I.Ch.E. Meeting, Washington (November 1969).
- A. M. Squires, C. A. Johnson, "The H-Iron Process", Journal of Metals, Vol. 9, 586-590 (1957).
- A. M. Squires, "Steelmaking in an Industrial Complex", Oak Ridge National Laboratory Report ORNI-4294, (November 1968a).
- A. M. Squires, "Iron and Steel with Hydrogen", Atomic Energy Commission Symposium Series, Vol. 14, 181-196 (Conf.-680810) (May 1969c).
- A. M. Squires, "Steam-Oxygen Gasification of Fine Sizes of Coal in a Fluidized Bed at Elevated Pressure", Trans. Inst. of Chem. Eng. (London), Vol. 39, 3-27 (1961).
- F. M. Stephens, Jr., W. M. Goldberger, "Combustion of Carbonaceous Solids", U. S. Patent 3,170,369 (March 2, 1965).

- S. Vecci, Babcock and Wilcox, Alliance Research Center, Alliance, Ohio, discussions with M. J. Gluckman and J. H. Siegell (August 1973).
- J. D. Watt, BCURA Industrial Laboratories, Leatherhead, England, "The Physical and Chemical Behavior of the Mineral Matter in Coal Under Conditions Met in Combustion Plant", (August 1969).
- J. Yerushalmi, M. Kolodney, R. A. Graff, A. M. Squires, R. D. Harvey, "Agglomeration of Ash in Fluidized Bed Gasifying Coal: The Godel Phenomena", Science, vol. 187, 646-648 (1975).

Vita

Jeffrey Howard Siegell was born in Brooklyn, New York, on January 3, 1950. He received his elementary and secondary education in the New York City Public School System. He entered Queensborough Community College, CUNY, in September 1968 and received the Associate of Science degree in Pre-Engineering in 1970. Transferring to the City College of New York he completed his Bachelors Degree in Chemical Engineering in 1973.

He then entered the doctoral program in Engineering at the City University of New York and worked as part of a research team engaged in a project to improve the techniques to gasify coal. He received his Master of Engineering(Chemical) in June 1974 and Doctor of Philosophy in June 1976.

Jeffrey Howard Siegell is a member of the American Institute of Chemical Engineers, Tau Beta Pi, Tau Alpha Pi, and Phi Theta Kappa.